Link Adaptation of Mobile Communication Networks with Limited Feedback Channels

Noha Alaa El-Din Abou Aly

MSc. Thesis

December 2015

A thesis submitted to Khalifa University of Science, Technology and Research in accordance with the requirements of the degree of Master of Science by Research in Engineering in the Department of Electrical and Computer Engineering.

Link Adaptation of Mobile Communication Networks with Limited Feedback Channels

by

Noha Alaa El-Din Abou Aly

A thesis submitted in partial fulfillment of the
requirements for the degree of

Master of Science by Research in Engineering
(Electrical & Computer Engineering)

at

Khalifa University

Thesis Committee

Dr. Arafat Al-Dweik (Supervisor),
Khalifa University

Dr. Mohamed Al-Mualla (Co-Supervisor)
Khalifa University

Prof. Xuemin (Sherman) Shen (External Examiner & Committee Chair),
University of Waterloo, Canada

Dr. Sami Muhaidat (Internal Examiner)
Khalifa University

December 2015

ABSTRACT

Noha A. Abou Aly, "**Link Adaptation of Mobile Communication Networks with Limited Feedback Channels**", M.Sc. Thesis, M. Sc. by Research in Engineering, Department of Electrical and Computer Engineering, Khalifa University of Science, Technology and Research, United Arab Emirates, December 2015.

This thesis considers end-to-end performance evaluation of wireless communication networks with link adaptation where orthogonal frequency division multiplexing (OFDM) is incorporated. In particular, the thesis focuses on evaluating the performance of adaptive wireless networks with limited feedback channels. Moreover, we consider imperfect feedback information where the feedback information might be erroneous or outdated due to the channel variations over time. The end-to-end performance considers the channel estimation errors in the feedforward channel and the noise and fading in the feedback channel. The thesis presents the performance of several adaptive techniques that are particularly designed for OFDM. The system and channel models are based on the state-of-the-art adaptive standards such as WiMAX.

The thesis also presents a new adaptive OFDM system for limited feedback channels. The proposed system is designed to minimize the number of feedback bits sent to the transmitter by sending a quantized and truncated version of the estimated channel impulse response. The proposed limited feedback technique depends on time-domain vector of the channel state information (CSI) instead of the corresponding frequency-domain vector in order to reduce the feedback overhead.

Indexing Terms: Adaptive modulation, OFDM, channel estimation, limited feedback channels, delay.

ACKNOWLEDGMENT

First and foremost, I am grateful to God for the good health, wellbeing and protection that were necessary to complete this thesis.

I would like to thank my family, who I have been blessed with, for their endless love and their priceless care and advice they provided me through my entire life and in particular through my M.Sc study. Without their care, encouragement and editing assistance, I would not have finished this thesis.

I am so grateful to the committe and faculty of graduate studies of Khalifa University for making it possible for me to study here. I would like to express my sincere gratitude to my supervisor Dr. Arafat Al-Dweik who has supported me during my M.Sc study with his valuable guidance, efforts and patience. His immense knowledge and expertise supported me all the time throughout my research and helped to enrich the experience. Also, I would like to express sincere thanks to Dr. Mohammed Al-Mualla for his appreciated encouragement, help and support during my graduate program. Special thanks goes to Dr. Mahmoud Al-Qutayri for the assistance he provided, and advice at times of critical need. My thanks extend to my examiners Dr. Sami Muhaidat and Prof. Xuemin (Sherman) Shen for their efforts and valuable feedback.

I doubt that I will ever be able to express my appreciation fully, but I owe them a deep sense of gratitude.

DECLARATION AND COPYRIGHT

Declaration

I declare that the work in this thesis was carried out in accordance with the regulations of Khalifa University of Science, Technology and Research. The work is entirely my own except where indicated by special reference in the text. Any views expressed in the thesis are those of the author and in no way represent those of Khalifa University of Science, Technology and Research. No part of the thesis has been presented to any other university for any degree.

Author Name: Noha Alaa El-Din Abou Aly.

Author Signature: _____

Date: _____

Copyright ©

TABLE OF CONTENTS

Page

LIST OF TABLES

Table **Page**

LIST OF FIGURES

Figure **Page**

LIST OF ABBREVIATIONS

AMS	Adaptive Modulation Selection
APA	Adaptive Power Allocation
ASK	Amplitude Shift Keying
ASCS	Adaptive Subcarrier Selection
AWGN	Additive White Gaussian Noise
BER	Bit Error Rate
BSC	Binary Symmetric Channel
CP	Cyclic Prefix
CSI	Channel State Information
DAB	Digital Audio Broadcast
DL	Downlink
DVB	Digital Video Broadcast
FDF	Frequency-domain Feedback
FEQ	Frequency-domain Equalizer
FFT	Fast Fourier Transform
FUSC	Fully used Subcarriers
ICI	Inter Carrier Interference
IEEE	Institute of Electrical and Electronics Engineers
IFFT	Inverse Fast Fourier Transform
ISI	Inter Symbol Interference
LAN	Local Area Network
LOS	Line-of-Sight
LTE	Long Term Evolution
MIMO	Multiple-Input Multiple-Output
M-QAM	M-order Quadrature Amplitude Modulation

MMSE	Minimum Mean Square Error
NMSE	Normalized Mean Aquare Error
OBF	One-bit per subcarrier feedback
OFDM	Orthogonal Frequency Division Multiplexing
PHY	Physical Layer
PUSC	Partially used Subcarriers
QPSK	Quadrature Phase Shift Keying
Rx	Receiver
SER	Symbol Error Rate
SNIR	Signal to Noise and Interference Ratio
SNR	Signal to Noise Ratio
TDF	Time-domain Feedback
TU	Typical Urban channel
Tx	Transmitter
UL	Uplink
WiMAX	Worldwide Interoperability for Microwave Access
WLAN	Wireless Local Area Network

LIST OF SYMBOLS

b_q	Number of quantization bits
E_b/N_0	Ratio of Bit energy to noise power spectral density
E_s/N_0	Ratio of symbol energy to noise power spectral density
f_c	Carrier frequency
f_d	Doppler spread
F_d	Normalized Doppler spread
f_s	Sampling Frequency
$\mathbf{H}$	$N \times N$ channel frequency response matrix
K	Number of OFDM symbols
L	Number of paths in multipath channel
N	Number of subcarriers in OFDM symbol
N_{p}	Number of pilots in OFDM symbol
N_{cp}	Number of CP samples in OFDM symbol
p	probability of error in BSC
p_{f}	Pilot symbols separation in frequency domain
t_{max}	Maximum excess delay
T_s	Sample period
T_{sym}	OFDM symbol period
Δf	Sub-Carrier Frequency Spacing

CHAPTER 1

INTRODUCTION

1.1 Motivation and Objectives of the Thesis

Wireless communication networks are currently facing rapidly increasing demands for reliable and high data rate transmission. The key solution to achieve such conflicting parameters is to dynamically adapt the system parameters based on the channel quality, traffic conditions and user requirements [1] to satisfy particular constraints such as bit error rate (BER), data rate, throughput, bandwidth or energy consumption. System parameters that are typically adapted at the physical layer (PHY) include transmission power, data rate, modulation and coding schemes. Generally speaking, satisfying most of the system requirements in static channels is straightforward and can be performed at the initial system setup process. However, the scenario is substantially different when the channel is changing rapidly over time, because the system parameters, during a particular transmission session, will be no longer optimal in the next session. Therefore, system adaptation is essential to track channel variations and optimize the network parameters accordingly. The adaptation process is a fundamental element in current wireless networks [2] (e.g., IEEE 802.11, IEEE 802.16, DAB, DVB, etc.) and the future networks as well [3]. For example, 5G networks have engouraged intensive research and development efforts on link adaptation processes [4], due to the growth of data traffic and shortage of spectrum.

In adaptive communication systems, specifying the transmission parameters can be performed at the transmitter or the receiver side. In both cases, the receiver has to feed back particular information to the transmitter. If the adaptation process is performed at the receiver side as in [5], the feedback information will comprise the transmission parameters

such as the power allocation and modulation values. If the adaptation is performed at the transmitter side [6], the receiver should send the channel state information (CSI) to the transmitter where it will use such information to select the appropriate system parameters. Choosing one approach over the other depends on the processing power of both devices and on the available power and bandwidth of the feedback channel. Usually, the feedback channel has power and bandwidth constraints which limit the feedback rate. Therefore, minimizing the number of bits sent over the feedback channel is consistently desired to reduce the overhead cost of the adaptation process. In this thesis, end-to-end performance evaluation for link adaptation OFDM wireless system is presented and a new feedback technique is proposed to limit feedback overhead and maintain a high performance adaptive communication system.

On the other hand, CSI should be available at the receiver side through channel estimation in order to have the adaptation information that is fed back from the receiver to the transmitter. In high mobility environments and due to the time variance and frequency selectivity of wireless channels, channel estimation is considered as a challenging problem in wireless systems. Therefore, channel estimation gained an essential concern in designing the receiver of OFDM systems to have successful link adaptation.

1.2 Contributions

One of the main contributions of the thesis is developing a new feedback overhead reduction technique using the time-domain CSI instead of its corresponding frequency domain vector, where a truncated and quantized version of the channel impulse response is fed back to the transmitter. The total overhead size is limited to N bits. where N is the number of subcarriers. Consequently, the average number of bits per subcarrier is one bit. At the transmitter side, the channel frequency response across all subcarriers can be achieved efficiently using FFT.

The thesis is also concerned with end-to-end performance evaluantion where the proposed feedback technique is tested over a feedback channel that is assumed to be an erroneous

and outdated channel. The quantization of the feedback vector of the channel information also gained a great concern in evaluation, where the performance is tested over a range of quantization bits number. Pilot-aided channel estimation technique is used over a static and mobile frequency selective channel and its impact on the system performance is studied. The performance of the proposed time domain feedback technique is tested in a link adaptation algorithm where the modulation order of each of the OFDM subcarriers is adapted according to Bit error rate (BER) constraints. The proposed feedback scheme is compared to several feedcack techniques and its performance is proved to outperform the other techniques in terms of throughput and BER while maintaining low feedback overhead.

1.3 Thesis Outline

This thesis is organized as follows:

Chapter 2 presents the OFDM system model and the mathematical representation of the data transmission and reception. It also presents the wireless channel model as well as the system parameters. Channel estimation specifications are provided in this chapter as well.

Chapter 3 gives an overview of link adaptation in wireless OFDM systems and specially adaptive modulation and adaptive power techniques. It also presents a detailed explanation to the adaptive modulation algorithm used in the thesis.

Chapter 4 covers channel state information (CSI) feedback techniques in wireless OFDM systems. The proposed time domain feedback technique is presented in this chapter. And an end-to-end performance evaluation is also shown. The evaluation includes CSI error distribution over a range of SNRs in feedforward and feedback channels. It also includes the effect of feedback information quantization as well as the probability of error in feedback channel on the feedback quality.

Chapter 5 provides an evaluation for the performance of the adaptive modulation algorithm using the proposed truncated channel impulse response feedback technique. It also

shows a performance comparison between the proposed feedback technique and other techniques presented in literature.

Chapter 6 covers the summary of the thesis and the conclusions and it ends the thesis with some possible ideas for the future work.

CHAPTER 2

OFDM SYSTEM AND CHANNEL MODELS

2.1 OFDM System:

This work consideres an OFDM system with N subcarriers. The data bits are mapped to N symbols, each is adaptively modulated with M-QAM (Quadrature Amplitude Modulation). The transmitted symbols are fed into N-point Inverse Fast Fourier Transform (IFFT) to perform the orthogonal modulation of the subcarriers. Block diagram of the system model is shown in Fig. 2.1. The transmitted OFDM symbol is formed by adding N_{cp} samples as a cyclic prefix to prevent inter-symbol-interference (ISI). The length of the cyclic prefix is chosen to be larger than the maximum delay spread of the channel. The transmitted baseband n-th sample in the i-th OFDM symbol is given by

$$x_i(n) = \frac{1}{N} \sum_{m=0}^{N-1} X_i(m) e^{-j\frac{2\pi mn}{N}} \tag{2.1}$$

where $X_i(m)$ is the complex valued data at the m-th subcarrier in the i-th OFDM symbol. The duration of the OFDM symbol is $T_{sym} = (N + N_{\text{cp}})T_s$, where T_s is the sample duration. The signal is then transmitted through a multipath Rayleigh fading channel. The frequency selective fading channel with L delay taps has impulse response that is described by:

$$h(t) = \sum_{l=1}^{L} c_l(t)\delta(t - \tau_l) \tag{2.2}$$

where $c_l(t)$ is the normalized gain of the l-th path which is a random variable with Rayleigh distribution, τ_l is its propagation delay, δ is the Dirac delta function and $\sum_{l=1}^{L} c_l(t) = 1$.

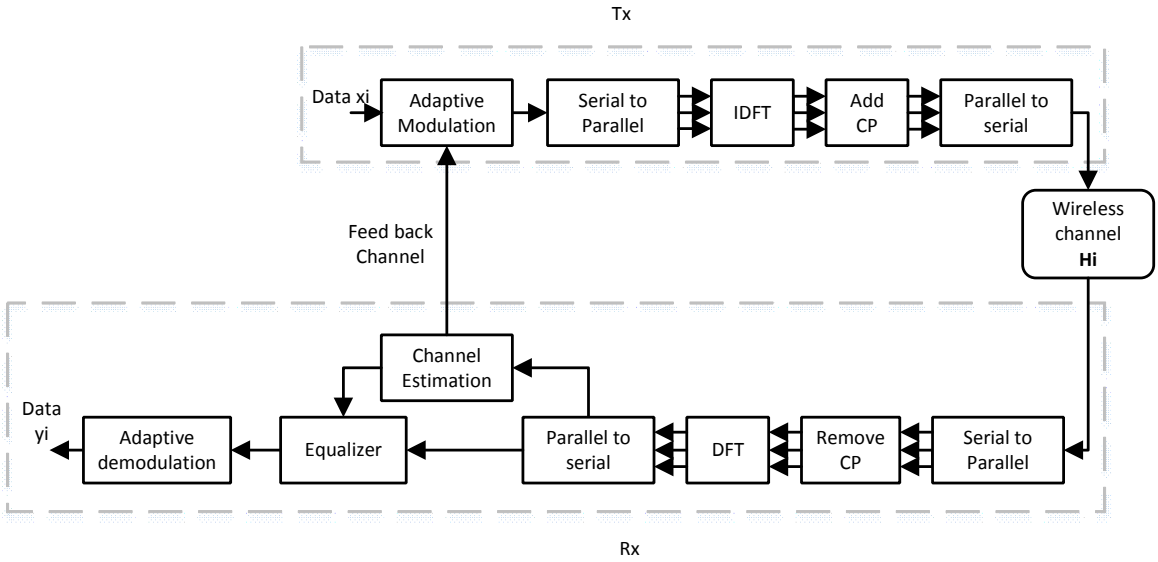

Figure 2.1. Block diagram of the system model.

Frequency and time synchronization are assumed to be perfect. After removing the CP, the received signal is represented as:

$$y_i(n) = \sum_{l=0}^{L-1} h_i(l;n)x_i((n-l)_N) + w_i(n) \tag{2.3}$$

where $h_i(l;n)$ represents the channel l-th tap at the n-th sample in the i-th OFDM symbol, $w_i(n)$ denotes additive white Gaussian noise (AWGN) with zero mean and variance σ_w^2, and $(.)_N$ is for representing a cyclic shift with base N. After FFT at the reciver, the received signal is

$$\mathbf{Y}_i = \mathbf{H}_i\mathbf{X}_i + \mathbf{W}_i \tag{2.4}$$

where $\mathbf{H}_i$ is the $N \times N$ channel matrix that represents the channel frequency response, $\mathbf{X}_i$ and $\mathbf{W}_i$ denote the transmitted data vector and AWGN, respectively. In static channels $\mathbf{H}_i$ is a diagonal matrix,

$$H_i(k,k) = \sum_{l=0}^{L-1} h_i(l)e^{-j\frac{2\pi}{N}lk} \tag{2.5}$$

In mobile channel, unlike the static channel, the channel matrix is no longer diagonal. The off-diagonal and diagonal elements in the channel matrix $\mathbf{H}_i$ are respectively [7]

$$H_i(k,d)=\frac{1}{N}\sum_{n=0}^{N-1}\sum_{l=0}^{L-1}h_i(l;n)e^{-j\frac{2\pi}{N}lk}e^{-j\frac{2\pi}{N}(d-k)n} \tag{2.6}$$

where $0 \leq k,d \leq N-1, k \neq d$

$$H_i(k,k)=\sum_{l=0}^{L-1}h_i^{avg}(l)e^{-j\frac{2\pi}{N}lk} \tag{2.7}$$

where $h_i^{avg}(l) = \frac{1}{N}\sum_{n=0}^{N-1}h_i(l;n)$.

At the receiver side, a zero-forcing single-tap equalizer is applied to the FFT output to equalize the received data. The zero-forcing equalizer satisfies the condition

$$\mathbf{G}_i\mathbf{H}_i = \mathbf{I} \tag{2.8}$$

where $\mathbf{G}_i = (\mathbf{H}_i^H\mathbf{H}_i)^{-1}\mathbf{H}_i^H$ is the zero-forcing decoding matrix, $\mathbf{I}$ is the identity matrix and $(.)^H$ is the Hermitian transpose. When $\mathbf{H}_i$ is a nonsingular matrix, $\mathbf{G}_i = \mathbf{H}_i^{-1}$.

The equalized data sequence is expressed as

$$\widehat{\mathbf{y}}_i=\mathbf{G}_i\mathbf{Y}_i. \tag{2.9}$$

2.2 WiMax Symbol Structure:

In WiMax standard, active data and pilot sub-carriers are grouped into subchannels which are subsets of sub-carriers. Sub-channelization is supported by WiMAX OFDMA PHY downlink (DL) as well as uplink (UL). A slot is formed of 48-subcarriers, which is the minimum sub-channelization unit. Subcarrier allocation scheme can be fully used subcarriers (FUSC) scheme and partially used subcarrier (PUSC) scheme.

In DL PUSC, for each pair of OFDM symbols, the active sub-carriers are grouped into clusters, each has 14 sub-carriers per symbol period. A re-arranging scheme is used to form

groups of clusters. Each group consistes of 2 clusters with 48 data subcarriers and 8 pilot subcarriers. Only pilot allocations in each cluster are shown in Fig. 2.2 [2] [8].

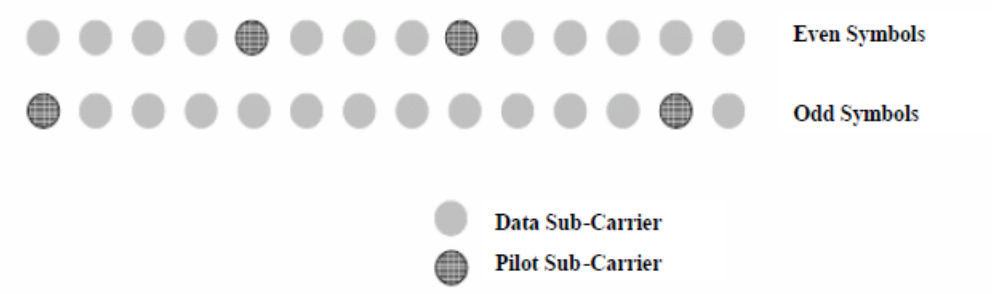

Figure 2.2. DL pilot allocation.

Similar to the difinition of cluster in DL, a tile structure is described for the UL (see Fig. 2.3) [2] [8]. Tiles are grouped together to form a slot. One slot contains 48 data sub-carriers and 24 pilot sub-carriers in 3 OFDM symbols. Mobile WiMax Parameters for UL and DL are shown in Table 2.1 [2] [8]

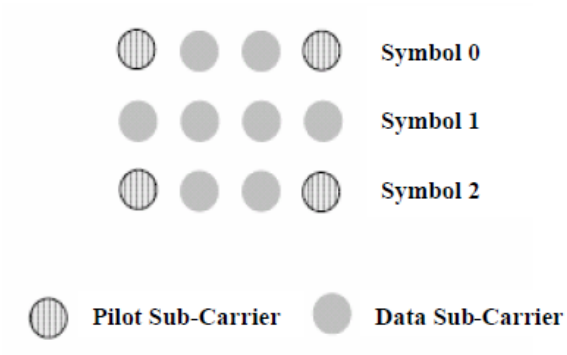

Figure 2.3. UL pilot allocation.

2.3 System Parameters:

The parameters of mobile WiMax (802.16e) standard are adopted. Table 2.2 shows the specifications of the system [2], [8].

Table 2.1. Mobile WiMax Parameters

Parameter	**DL**	**UL**	**DL**	**UL**
System Bandwidth	5 MHz		10 MHz	
FFT size (N)	512		1024	
Null Sub-Carriers	92	104	184	184
Pilot Sub-Carriers	60	136	120	280
Data Sub-Carriers	360	272	720	560
Sub-Channels	15	17	30	35
OFDM Symbol duration	102.9 μs			
Frame Duration	5 ms			
OFDM Symbols/Frame	48			
Data OFDM Symbols	44			

Table 2.2. Specifications of the System

Parameter	**Value**
System Channel Bandwidth	5 MHz
FFT size (N)	512
Sampling Frequency (fs)	5.6 MHz
Useful Symbol duration (T_{sym})	91.4 μs
Cyclic Prefix (CP)	1/8
OFDM Symbol duration	102.9 μs
Sub-Carrier Frequency Spacing (Δf)	10.94 kHz
Pilot Separation	5

Table 2.3. 6-Taps Typical Urban Channel.

Tap no.	**Relative Delay (μs)**	**Average Power (dB)**
1	0	-3
2	0.2	0
3	0.5	-2
4	1.6	-6
5	2.3	-8
6	5	-10

The OFDM signal is transmitted through a multipath Rayleigh fading channel, where the channel model is 6-taps Typical Urban (TU) channel profile. The frequency selective fading channel has an impulse response with 6 paths. Each path has different delay and relatively strong power as shown in Fig. (2.4). The average power and the delay of each path are given in table (2.3) [9][10].

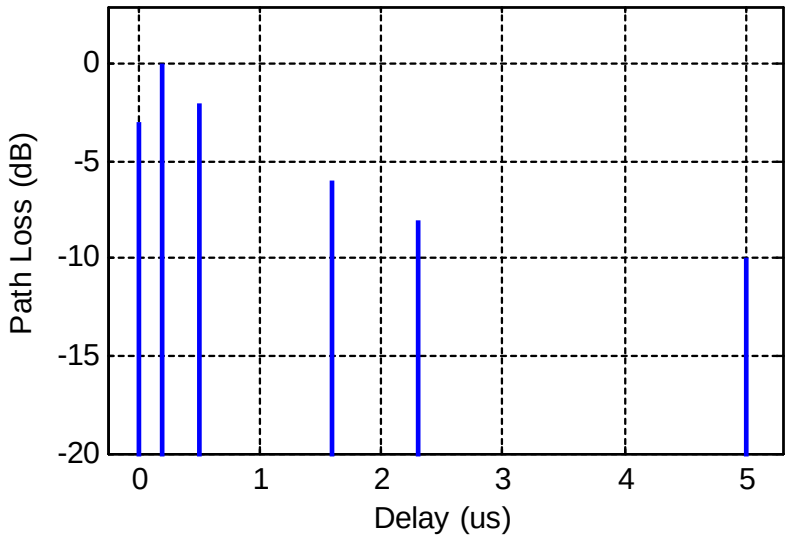

Figure 2.4. TU-6 channel impulse response.

2.4 Channel Estimation (Related Work):

The channel estimation considered in this thesis is based on pilot symbols. This section shows the impact of the pilot spacing used for channel estimation on BER and it is evaluated under different channel conditions. BER is evaluated with perfect and imperfect channel estimation. The imperfect channel estimates are obtained by using pilots with different densities at different operating conditions.

The transmitted and received j^{th} pilot subcarrier in frequency domain are denotted as $X_p(j)$ and $Y_p(j)$ respectively. The estimated channel frequency response at the pilot subcarriers is represented as:

$$\widehat{H}_p(j) = \frac{Y_p(j)}{X_p(j)} \tag{2.10}$$

$$= H_p(j) + W_p + \Phi_p \ , \ j = 0, 1, .., N_p - 1 \tag{2.11}$$

where $H_p(j)$ is the actual channel frequency response at the pilot subcarriers, W_p is AWGN and Φ_{np} is the interference term that can be approximated by a Gaussian distribution [35] at pilot subcarriers because the interference and noise distribution after dividing by the data symbols retains the same Gaussian approximation.

To estimate the channel at data subcarriers, interpolation technique among pilot subcarriers is required. Channel interpolation can be performed using linear, second order, low-pass, cubic spline, or time domain interpolation. The estimated channel frequency response at the m^{th} subcarrier is represented as:

$$H_e(m) = H(m) + I(m) \tag{2.12}$$

where $I = W + \Phi + P$. The interpolation error is denoted as P and I is the estimation error vector. According to the simulation results I can be approximated by a Gaussian distribution with zero mean and σ_I^2 variance as illustrated in section 4.2.

2.4.1 Pilot Grid Design:

In general, pilot grid can be block-type or comb-type pilot arrangement. In block type arrangement, pilots are placed in every subcarrier in OFDM symbols every a specific time period. While, in comb-type-pilot arrangement, the pilot subcarriers are placed in each OFDM symbol at different positions in the frequency grid [11] as shown in Fig. 2.5. In time varying channels, variations of the channel gains over OFDM symbols are non-negligible. Therefore, in order to have more accurate channel estimation, comb-type-pilot arrangement is prefered in this work.

In order to recover the CSI accurately, the pilot symbols grid density must satisfy the 2-D sampling theorem as discussed in [12]:

$$p_{\mathrm{f}} \leq \frac{1}{2t_{\max}\Delta f} \quad \text{and} \quad p_{\mathrm{t}} \leq \frac{1}{2f_{\max}T_{sym}} \tag{2.13}$$

where p_{f} and p_{t} denote the spaces between pilots in frequency and time domain respectively. $t_{\max}$ is maximum excess delay of the channel and Δf is subcarrier spacing. $f_{\max}$ denotes the maximum doppler frequency and T_{sym} in the symbol duration. In order to have highly accurate channel estimation, pilot symbols grid is oversampled by a factor of two [12]. In this work, comb-type-pilot arrangement is adopted, where N_{P} pilot subcarriers are transmitted every p_{f} subcarriers within each OFDM symbol.

2.4.2 Interpolation:

To estimate the channel at data subcarriers, interpolation techniques of the estimated channel response at pilot subcarriers among the frequency grid is required. Channel interpolation can be done using linear interpolation, second order interpolation, low-pass interpolation, cubic-spline interpolation, and time domain interpolation. In this work, cubic spline interpolation is adopted because of its reliable performance [13]. Cubic-spline interpolation method is based on drawing smooth curves through a number of points, which produces a continuous polynomial fitted to given data points [13].

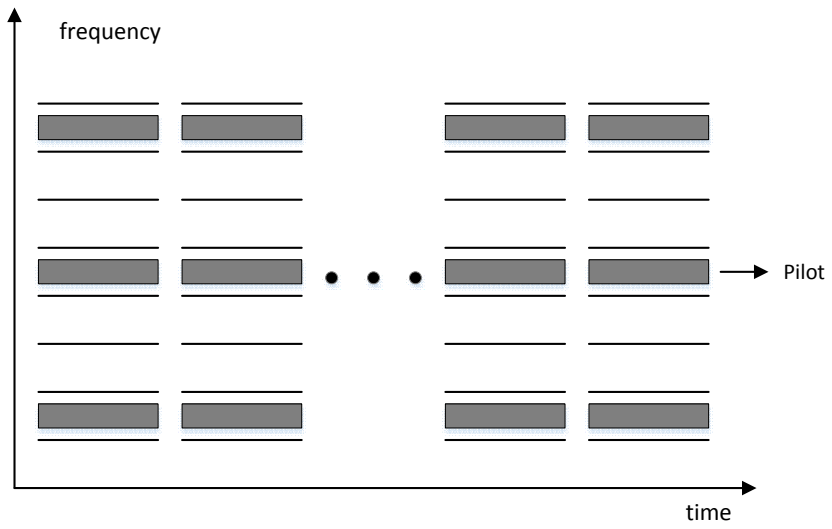

Figure 2.5. Comb-type-pilot arrangement.

2.4.3 Numerical Results

Fig. 2.6 illustrates the effect of pilot separation (p_{f}) on the BER of the OFDM system with QPSK modulation where the channel model is 6-taps TU static channel. In general, degradation in BER occures with the increase of pilot separation. The simulation results support the idea of pilots grid density that is discussed earlier in Section 2.3.1. According to the system model parameters, pilots separation in the frequency grid is

$$p_{\mathrm{f}} \leq \frac{1}{2t_{\max}\Delta f} = \frac{1}{2 \times 5\mu s \times 10.94kHz} = 9.14 \tag{2.14}$$

and oversampling pilot symbols grid by a factor of two gives that $p_{\mathrm{f}} \leq 4.57$.

The figure shows that for pilot spacing smaller than 5 subcarriers, the improvement in the CSI estimation quality is not significant. Therefore, using pilot spacing smaller than 5 subcarriers can cause a loss in the throughput without having a significant improvment in the channel estimation. For p_{f} greater than 5 subcarriers, the impact of the degradation in CSI estimation becomes noticeable at high SNR where error floors start to appear. At a certain stage, if the pilot spacing is relatively high, increasing the SNR will not improve the

performance, where the effect of the errors caused by interpolation between pilot subcarriers appears significantly.

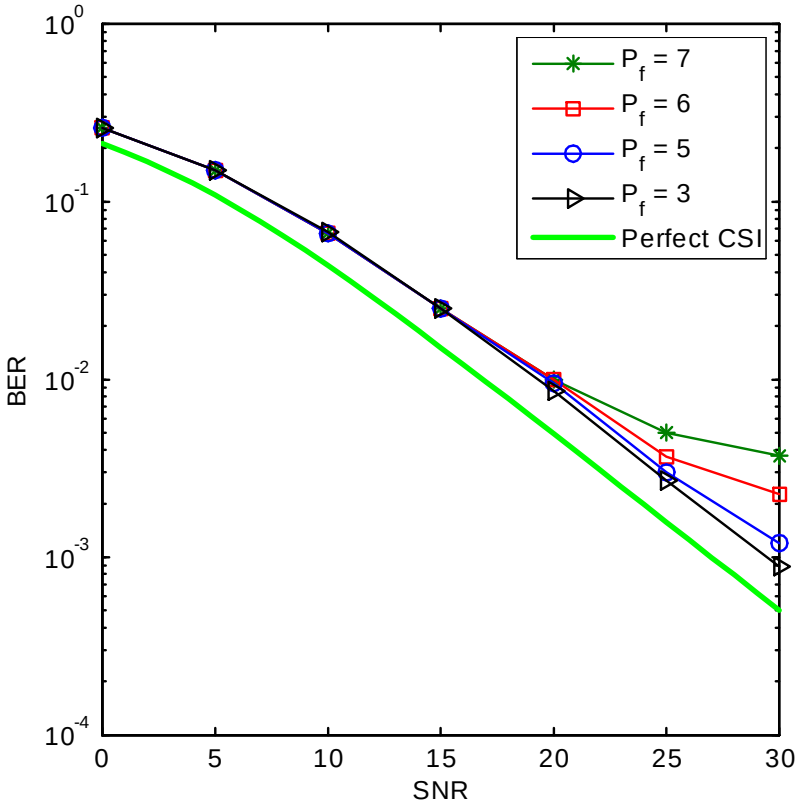

Figure 2.6. BER vs SNR, with different p_{f} values.

CHAPTER 3

LINK ADAPTATION TECHNIQUES IN WIRELESS OFDM SYSTEMS

3.1 Introduction

When the wireless signal is transmitted through multipath fading channel, its quality degrades and the BER increases a lot. Due to frequency selective fading channels, each one of the subcarriers in the OFDM signal can be affected by different channel gain and each one will have different SNR value. The performance of communication through wireless channel can be significantly improved through link adaptation. Once the channel state information of each subcarrier is known, different number of bits i.e. different modulation modes are assigned to different subcarriers according to these channel conditions and some specified constraints. This process is called bit loading (ex.[14]-[18]). Another form of link adaptation is called power loading (ex. [19]-[23]) where the transmission power is distributed among subcarriers according to their corresponding channel conditions as well as transmission constraints. [24].

In general, bit and power loading have two main aims. The first one is to maximize the system margin. In other words, to minimize transmission power subjects to a target data rate. The second aim is to maximize the system data rate. To achieve these goals, some algorithms depend on greedy techniques for data filling and data removal. Such techniques allocate discrete number of bits for each subcarrier directly until the target BER value is achieved, so it converges slowly [25]. Algorithms that employ greedy bit filling and greedy bit removal proved their success in bit loading, but they suffer from computational complexity

during operations for searching for maximum and minimum bits values. The authors in [26] proposed bit loading algorithm that is a 3 step process that proved its optimality, but unfortunately it still suffers from complexity that is dominated by the greedy filling and removal processes.

Other algorithms use a technique called water filling, in which a non-integer number of bits are allocated to subcarriers followed by a step for assigning discrete number of bits to each one. Water filling algorithm works by giving more power to subcarriers that have higher SNR and vice versa [25]. In [14] two stage bit loading algorithms are proposed. Efficient Bit Filling (EBF) and Efficient Bit Removal (EBR) algorithms are proposed based on group by group bit filling/removal algorithm that depends on greedy bit filling and greedy bit removal. EBF and EBR are aiming at reducing the transmit power to achieve a specific data rate, BER, constraints of maximum power for each subcarrier and the maximum allowable constellation's size. The complex channel gain and the SNR values are determinants to the number of bits that have to be assigned to each subcarrier. Iterative group by group bit loading algorithms are presented in [15]. Refined greedy bit removal (r-GBR) and refined greedy bit filling (r-GBF) algorithms are proposed where the group of bits for each subcarrier is adjusted dynamically in order to overcome the limitations of the greedy algorithms. In the two proposed algorithms, additional greedy bit filling or bit removal processes follow the group by group bit loading algorithm to force it to converge to optimal bit loading profile.

Authors in [16] proposed bit loading algorithm for maximizing the system throughput with BER constraints, while maintaining uniform power allocation. The maximum possible number of bits are loaded to each subcarrier so that its BER is bellow a maximum predefined value. The proposed algorithm has a comparable complexity when compared to other algorithms that employ water filling approximation. However, the throughput achieved is near to optimality. Author in [17] shows a draw back in an algorithm for bit loading in OFDM system. This algorithm depends mainly on the idea of sorting the subcarriers in which the complexity exist. Although the algorithm enjoyed success when used by other authors, the author of [17] claims that the algorithm is suboptimal and removed this drawback and extended it into an optimal algorithm by introducing a sufficient condition for an acceptable

power allocation. [18] proposed a bit loading algorithm that is able to converge to the same number of bits faster than discrete bit filling and removal algorithms. Multiple bit insertions and removal processes are done to achieve the aimed number of bits. The initial value for each subcarrier is determined according to the corresponding subchannel gain to noise ratio.

The proposed power loading algorithm in [19] is applied on constant data rate OFDM system and its target is to minimize the power used for transmission while meeting the BER constraints. The main idea of the algorithm depends on considering the unequal bit error rate among subcarriers. A closed form expression is derived for acheiving optimality in power allocation among subcarriers. [20] presents an iterative water filling power loading algorithm to improve the spectral efficiency while maintaining a target BER and a maximum transmit power allowed. According to the SNR for each subcarrier, bit rates are decided and the power is distributed among subcarriers, then the suitable modulation mode is decided according to the number of bits dedicated for each subcarrier. [21] presents water filling power loading algorithms for distributing power among subcarriers trying to maximize the system margin. Power allocation differs from one carrier to another mainly depending on the channel gain and the SNR of each subcarrier while it lets the bit allocation to be uniform. Authors claim that this algorithm outperforms others that use uniform power allocation and allow adaptive bits distribution. The introduced algorithm in [22] is an adaptive power allocation algorithm in OFDM system in which the power is distributed among subcarriers aiming to minimize the bit error rate considering the total power constraints. [23] presents a power loading algorithm that is claimed to outperform both of the water filling and the greedy algorithms. With the distribution of the power over parallel channels, it can increase the mutual information between them.

In [27], adaptive bit and power loading are considered in OFDM system. The main aim is minimizing BER and it is achieved by three adaptive schemes. The first one is adaptive power loading, where the optimal power allocation coefficients are achieved at invariable rates while meeting the total power constraints. The second algorithm is a bit loading algorithm, where the optimal constellation is decided for each subcarrier under rate constraints and invariable power coefficients. The third one is a joint bit and power loading algorithm. [28]

shows a study of bit and power loading for OFDM system in the presence of inter-carrier interference (ICI) as well as inter-symbol interference (ISI). To avoid the degradation of the system performance because of ISI and ICI, a greedy algorithm is applied as a proposed initial solution followed by several approaches with reduced computational complexity. In [25] non-iterative bit and power loading algorithms are proposed. They target increasing the system's throughput and minimizing the transmit power subject to BER constraints. The algorithm uses a closed form expression to adapt bit and power distribution among subcarriers according to the channel gain at each subcarrier in fading channels. The main idea depends on checking the channel-to-interference-plus-noise ratio for each subcarrier and if it fulfills the predefined conditions, each subcarrier gets its suitable amount of power, otherwise the subcarrier is nulled. The presented algorithm is claimed to outperform the algorithm in [16]. Also authors in [29] present bit and power allocation algorithm. The main idea behind the proposed algorithm is to calculate the total power among all subcarriers, and compare it to the total power available. If it is below the given value, this means that the power constraints are achieved. Otherwise, the number of bits of the subcarrier with the maximum power is reduced by one and the process is repeated if the power constraints are not met yet. The algorithm is claimed to outperform [16] with similar or lower computational complexity.

3.2 Adaptive Modulation Algorithm

This section introduces a discrete adaptive bit loading algorithm which is considered for OFDM system with uniform power allocation. The algorithm aims to maximize the spectral efficiency of the system under mean bit error rate constraints. The algorithm performance is evaluated under perfect and imperfect channel information. The effect of erroneous as well as outdated feedback channel on the algorithm's efficiency are also evaluated. The adaptive algorithm is the bit allocation algorithm introduced in [30]. The algorithm's target is to solve:

$$\max_{k_i} \sum_{i=1}^{N} k_i \text{ , subject to } \overline{BER} = \frac{\sum_{i=1}^{N} k_i BER_i}{\sum_{i=1}^{N} k_i} \leq BER_T \tag{3.1}$$

where k_i is the number of bits allocated to subcarrier i, BER_i is the bit error rate of the i-th subcarrier , $\overline{BER}$ is the average bit error rate and BER_T is the specified bit error rate constraints . BER_i is determined according to k_i and the SNR of the subcarrier . SNR of the i-th subcarrier is

$$\gamma_i = \frac{|H_i|^2 |s_i|^2}{\sigma_w^2} \tag{3.2}$$

where H_i is the channel gain and $|s_i|^2$ is the average power of the i-th subcarrier. σ_w^2 is the variance of the zero mean AWGN and it is

$$\sigma_w^2 = \frac{\text{avg. signal power}}{\overline{\gamma}} \tag{3.3}$$

where $\overline{\gamma}$ is the average SNR.

The possible modulation schemes in the system are QPSK, 16-QAM and 64-QAM. The bit error rate of QPSK is given by [31] :

$$BER_i = Q\left(\sqrt{2\gamma_i}\right). \tag{3.4}$$

While the bit error rate of rectangular M-QAM is given by [31] :

$$BER_i = \frac{4\left(1 - \frac{1}{\sqrt{M_i}}\right)}{\log_2 M_i} Q\left(\sqrt{\frac{3\gamma_i \log_2 M_i}{M_i - 1}}\right) \tag{3.5}$$

where $\log_2 M_i = k_i$.

The worst case computational complexity of the algorithms under study is of $O(N^2)$ [30]. At the begining of the algorithm, a modulation mode is assigned to each subcarrier according to its SNR value. A look up table is designed to decide k_i according to γ_i so that $BER_i \leq BER_T$ is acheived. Table (3.1) shows the look up table for $BER_T = 10^{-3}$.

Table 3.1. Modulation Order Lookup Table

$\gamma_i(dB)$	$\gamma_i < 9.5$	$9.5 \leq \gamma_i < 16.5$	$16.5 \leq \gamma_i < 22.5$	$\gamma_i \geq 22.5$
Modulation order	Subcarrier is nulled	QPSK ($k_i = 2$)	16-QAM ($k_i = 4$)	64-QAM ($k_i = 6$)

One way to fulfill the BER constraints is to assign different modulation mode to each subcarrier to set its instantaneous bit error rate below or equal to BER_T. At the same time, to maximize the spectral efficiency, it is possible to acheive an average bit error rate ($\overline{BER}$) below or equal to BER_T while some subcarriers have instantaneous BER above BER_T. The operation of this adaptive modulation algorithm is shown in Fig. 3.1 and it is described as follows:

1. for $i = 1 : N$
2. Compute γ_i using (3.2).
3. Set k_i according to table (3.1).
4. end
5. Compute $\overline{BER}$ according to (3.1).
6. while $\overline{BER} < BER_T$
7. for $i = 1 : N$
8. if $k_i \neq 6$
9. $k_i = k_i + 2$
10. Compute BER_i
11. $k_i = k_i - 2$
12. end
13. end

14. Select j (the index of the smallest BER_i above BER_T)

15. $k_j = k_j + 2$

16. Compute $\overline{BER}$ according to (3.1).

17. end

18. if $\overline{BER} > BER_T$

19. $k_j = k_j - 2$

20. end

Fig. 3.2 shows snapshots of the channel frequency response ($20\log_{10}|\mathbf{H}_i|$), SNR dB ($\gamma_i$) and the initial and the final bit allocation (k_i) of each subcarrier. CSI is assumed to be known perfectly at the transmitter.

Fig. 3.3 shows the spectral efficiency of the adaptive bit allocation algorithm obtained from simulations compared with the non-adaptive modulation over different average SNR values ($\overline{\gamma}$). In the non-adaptive modulation system, k_i does not differ from one subcarrier to the other and it is constant over time. According to [33] the maximum average throughput (bits/subcarrier/OFDM symbol) that can be acheived according to BER_T with non adaptive modulation is :

$$c = \log_2\left[\frac{1.6\overline{\gamma}}{\frac{0.2}{BER_T} - 1} + 1\right]. \tag{3.6}$$

3.3 Channel Model

The time-varying fading channel is generated based on Jakes' model [34], in which the time correlation function follows

$$\rho_d = J_0(2\pi f_d \Delta t) \tag{3.7}$$

where $J_0(.)$ is the zero-order Bessel function of the first kind, f_d is the maximum Doppler frequency and Δt denotes the time separation in samples. Fig. 3.4 shows the normalized

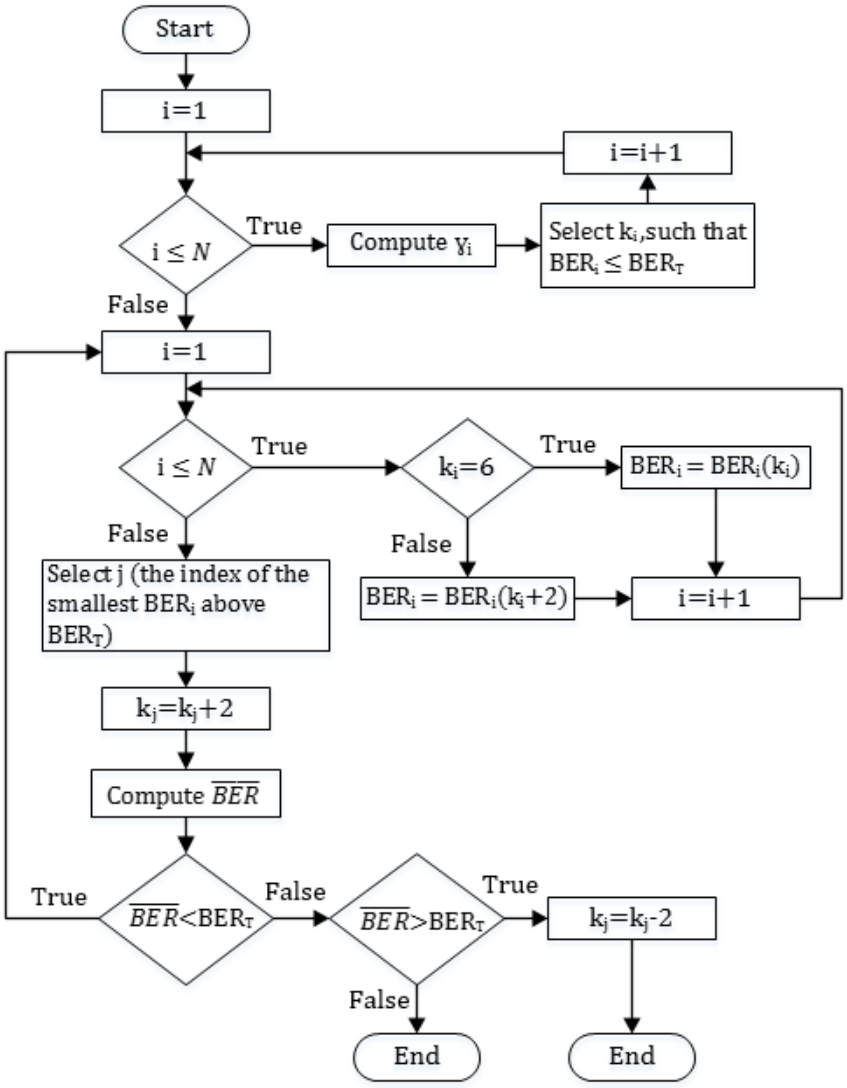

Figure 3.1. Flow chart of the adaptive modulation algorithm.

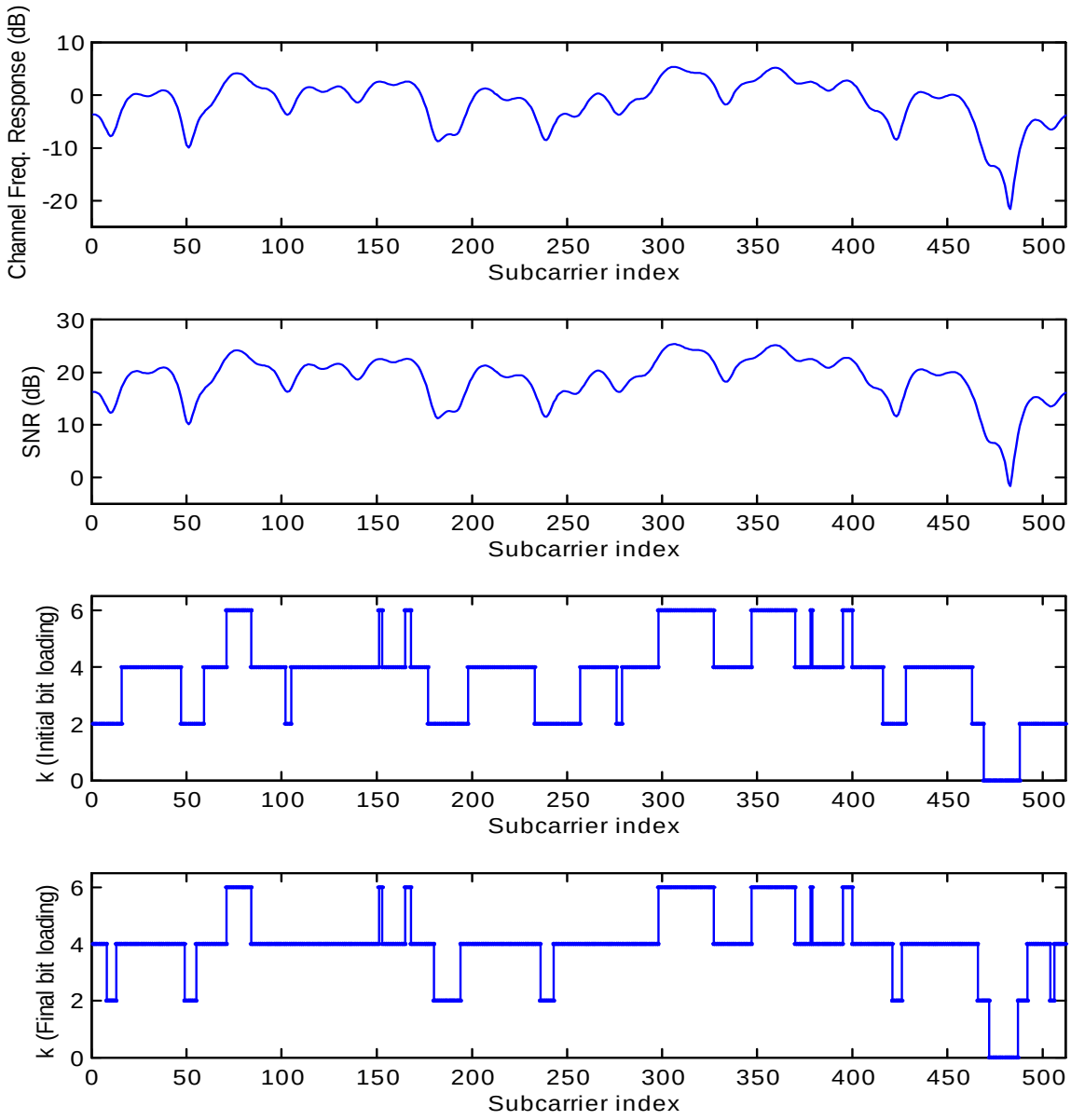

Figure 3.2. Snapshots of the channel frequency response, SNR (dB) of each subcarrier and the initial and the final bit allocation.

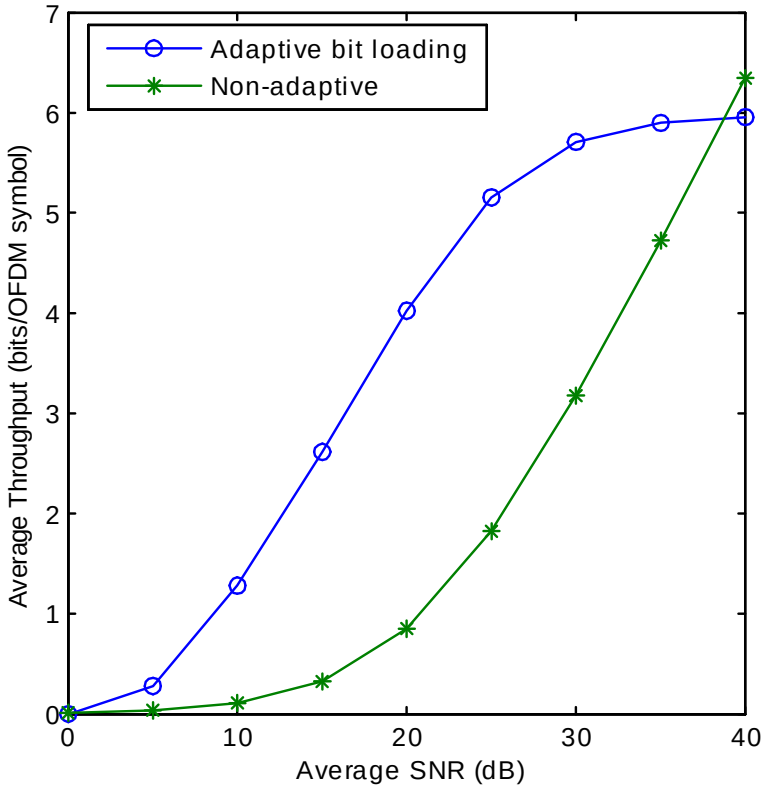

Figure 3.3. Average throughput of the adaptive modulation algorithm compared to non adaptive modulation.

CSI autocorrelation coefficient as a function of time separation in samples. The channel is assumed to be a mobile channel with normalized doppler $F_d = \{0.1, 0.01\}$. The correlation function used is given by:

$$\rho_d = E[H_n^* H_{n+\Delta t}] \tag{3.8}$$

where H_n is the channel gain at the n-th sample.

In static channel ($F_d = 0$), the channel is assumed to be constant over the duration of OFDM symbol, which makes the channel matrices diagonal. The mobile channel is unlike the static channel, where the channel matrices are no longer diagonal. Inter-carrier-interferense ICI is generated in this case as a result of the off-diagonal elements of the channel matrices

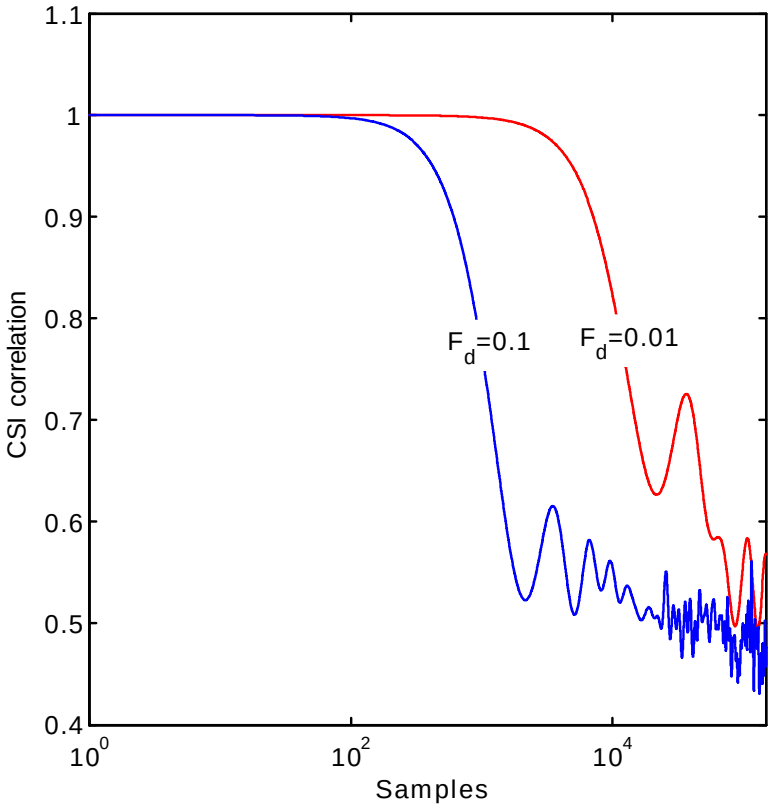

Figure 3.4. CSI correlation vs time separation is samples.

caused by the channel vairations within one OFDM symbol. Consequently, in mobile channel the adaptive modulation is affected by the intefrerence, therefore it is done depending on the subcarrier's SNIR, unlike the case of static channel where the adaptation depends on the SNR value.

The signal-to-noise and interference ratio (SNIR) at the i-th subcarrier is given by [35]:

$$SNIR_i = \frac{|s_i|^2}{\sigma_w^2 + E\left[|\Phi_n|^2\right]} \tag{3.9}$$

where $E\left[|\Phi_n|^2\right]$ is the ICI power, assuming that the elements of Φ_n approximately have Gaussian distribution with zero mean [35]. Depending on (3.7) the ICI power can be given by [35]:

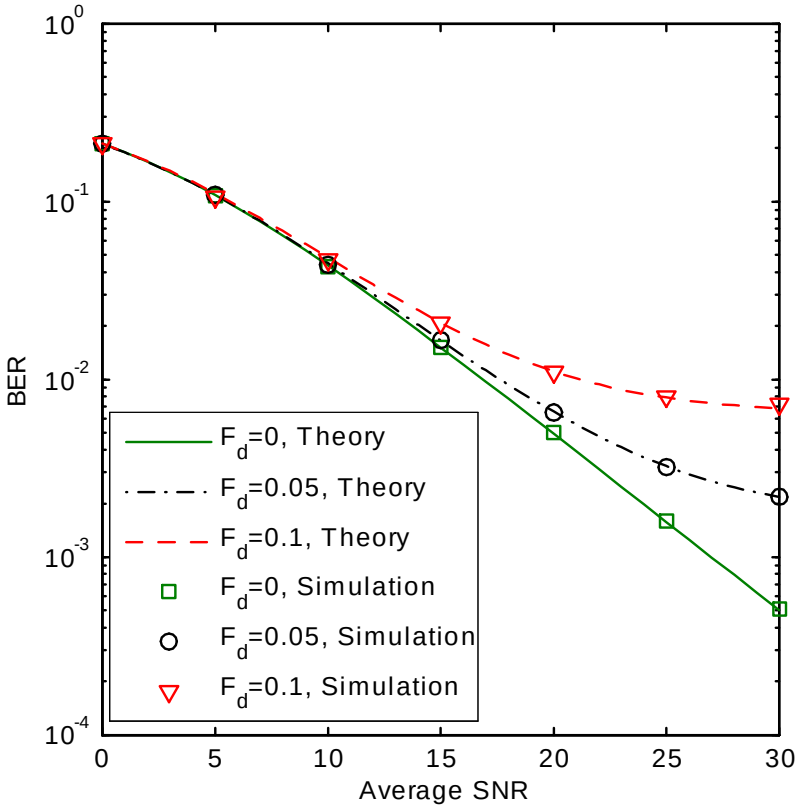

Figure 3.5. BER of QPSK modulation vs average SNR for different F_d values.

$$E\left[|\Phi_n|^2\right] = \sum_{n=0}^{N-1}\sum_{l=0}^{L-1}\sum_{i=0}^{N-1}\sum_{k=0}^{N-1}\frac{c_l}{N^2}J_0\left[2\pi f_d T_s\left(i-k\right)\right]e^{j2\pi n\frac{i-k}{N}} \tag{3.10}$$

where c_l is the normalized channel gain at l-th multipath component and T_s is the sample duration. $J_0(:)$ is the Bessel function of the first kind and zero order and f_d is the doppler shift. ICI will cause BER degradation as shown in Fig. 3.5 where QPSK is used for modulation and its BER is modified as:

$$BER_i = Q\left(\sqrt{2SNIR_i}\right). \tag{3.11}$$

And the BER of M-QAM is modified as:

$$BER_i = \frac{4\left(1-\frac{1}{\sqrt{M_i}}\right)}{\log_2 M_i}Q\left(\sqrt{\frac{3SNIR_i\log_2 M_i}{M_i-1}}\right). \tag{3.12}$$

CHAPTER 4

CSI FEEDBACK TECHNIQUES

In this chapter, an end-to-end system performance evaluation including several feedback techniques is studied. Also the evaluation of the system performance regarding imperfect channel estimation and imperfect CSI feedback is studied in several aspects. Normalized mean square error (NMSE) is used to quantify the difference between the actual CSI and the feedback CSI that is obtained from the feedback information. In this chapter, a proposed time domain feedback technique is presented and evaluated along with other feedback techniques in different forward and feedback channel conditions. Moreover, the effect of quantization on the NMSE between the actual and the feedback CSI is evaluated.

4.1 Introduction

In multicarrier wireless communication systems, link adaptation plays a vital role in optimizing the system performance. In order to have effective adaptation, the transmitter should have sufficient information about the wireless channel. Therefore, either CSI or link adaptation parameters are provided to the transmitter through feedback channels. However, the capacity of the feedback channel is usually limited, which makes the idea of reducing the feedback load a crucial one. Consequently, the feedback information reduction have received significant attention in the literature and will be discussed in the following paragraphs of this section.

In an effort to minimize the feedback overhead in OFDM systems, the authors in [36] proposed to feed back the channel time domain information instead of the frequency domain

CSI. Also, to reduce the errors occurring in the feedback channel, a robust precoder design is introduced on linear precoding as well as Tomlinson-Harashima precoding. The time-domain channel coefficients are quantized at the receiver side taking an advantage of the channel correlation. The performance of the proposed algorithm shows a reduction in the feedback overhead, but it is not evaluated over mobile fading channels. Channel estimation is assumed to be perfect and the quality of the feedback varies directly with the length of the compressed time-domain vector, which increases by the decrease of correlation in CSI. [37] and [38] propose a power loading algorithm over limited feedback channel. Both the transmitter and receiver are equipped with a code-book that has the possible quantized power vectors for all OFDM subcarriers and it is designed based on Lloyd algorithm. It is assumed that the destination gains full and perfect knowledge of the CSI, so it decides which power allocation vector is the suitable one and sends only its index in the available codebook to the transmitter through the feedback channel. Delay and imperfections in feedback channel are not considered.

The authors in [39] introduce an adaptive OFDM communication system where the transmitter receives only one bit per subcarrier through feedback which is achieved by dividing all CSI values into two groups only. The system parameters are designed according to IS-136 standard and channel estimation is assumed to be perfect. The adaptive techniques used in this system are: Adaptive Subcarrier Selection (ASCS), Adaptive Power Allocation (APA) and Adaptive Modulation Selection (AMS). BER is the only criterion used to evaluate the techniques performance. A similar technique is discussed in [40] for power allocation in multicarrier system using rate-distortion feedback codes. Due to the limited feedback information per subcarrier, the achieved throughput performance improvement in such techniques is limited.

Feedback overhead reduction using adaptive quantization is presented in [41]. According to the number of bits used in quantization, the suitable codebook is chosen from a set of predetermined codebooks. However, such methods suffer from a prohibitively high complexity. An adaptive codebook is also considered in [42]. That codebook adapts to different channel distribution, and it is built by both codebooks discussed in IEEE 802.16e: 16e codebook

and DFT codebook. It gains good performance in correlated and uncorrelated channels, but with an increase in feedback overhead, specially with the case of uncorrelated channels. A computationally efficient algorithm is proposed in [43], which exploits the correlation between subcarriers. The cardinality of the CSI are assumed to be finite and less than $Q = 2^{fb}$, where fb is the maximum number of feedback bits per fading block. However, the efficiency of such techniques degrades in response to the increase in delay spread.

The temporal and the spectral correlations are both used in a differential feedback scheme [44]. Authors in [44] used the 2-D correlation over selective fading channels and derived an expression for the minimal differential feedback rate. The transmitter predicts the current CSI depending on the previous CSI in the time-domain as well as the frequency-domain. After that, the receiver calculates the error in the channel state prediction (differential CSI) that is done by the transmitter and sends it through feedback channel to the transmitter. Then, the transmitter reconstruct the CSI utilizing the differential CSI and the channel prediction. Accordingly, reconstructing more accurate CSI reduces the number of bits in the feedback channel. However, when the correlation factor decreases, a significantly large feedback overhead is required.

In [6] and [45] the range of all the possible subchannel gains is divided into a finite number of regions and each region is assigned to a unique index. A number of pilots is used in [6] for channel estimation and at the receiver side each pilot subcarriers will be given an index according to the region that its gain belongs to. Then, the receiver will feedback these indices as well as the maximum and the minimum gain values to the transmitter. Letter [45] proposes a limited feedback scheme that is based on dynamic region. When the receiver receives all subcarriers, it can determine the value of the maximum as well as the minimum gain easily. Using these values, the range of all the possible subchannel gains is divided dynamically into a number of equal regions that are saved into a codebook. A number of pilots is used for estimating the channel gain at each subcarrier. At the receiver side, each subcarrier will be given an index according to the region that its gain belongs to. Then, the receiver will send these indices as well as the maximum and the minimum gain values to the transmitter through feedback channel that is asuumed to have neither errors nor

delay. Depending on the estimated channel gain at each subcarrier, the available transmit power will be distributed among them using water filling power allocation algorithm. The total amount of feedback overhead is $(2B + N_{\mathrm{p}} \log_2 E)$ bits, where $2B$ bits are required for maximum and the minimum gain values. So, feedback quality increases with the increase of E, on the expense of increase in the feedback overhead. However, in such techniques the feedback quality is acceptable only when the channel gains of all subcarriers are uniformly distributed between the maximum and the minimum values, which is not the case usually.

Paper [46] reviews algorithms for reducing limited rate feedback and divided them into three groups. The first one is called "Equally spaced subcarrier algorithms", in which the gain of a specific number of subcarriers is quantized by the receiver and sent back to the transmitter. The gain values of the rest of the subcarriers are estimated at the transmitter using interpolation techniques. The second group is "subcarrier grouping algorithms", in which the algorithms utilize the correlation between subcarriers. The correlated subcarriers in OFDM system are divided into groups. According to the gain that characterizes each group, it is defined by a certain index in a predefined codebook. "Subcarrier ordering algorithms" are the third group. In such algorithms, a code book that contains all the possible orders of the channel gains at pilot subcarriers is predefined and available at the transmitter and the receiver. The receiver feeds back to the transmitter the index of the channel gain's order at each pilot subcarrier and the quantized values of the maximum and the minimum gains. Then the gains of the remaining subcarriers are estimated by the transmitter using equally spaced method. A MIMO-OFDM system through a static multipath channel is considered in [47]. The proposed idea also depends mainly on dividing subcarriers into groups (chunks) and feedbacks information about each group only, aiming to reduce the amount of feedback overhead. Each one of these chunks contains a number of neighboring subcarriers and a number of consecutive OFDM symbols in frequency domain and time domain respectively. Choosing the optimized chunk size is done through a proposed optimistic scheme. Also, an approximation for the net throughput is considered. In order to decrease the amount of feedback overhead and to increase the net throughput in each chunk, users that have data rates below a certain threshold are not reported back to transmitter.

Delay and imperfections in the limitted feedback channel are not considered. However, such methods either do not accurately describe the actual characteristics of transmission channels, or cannot effectively cut down feedback overhead.

The work presented in [48] is based on assuming that the receiver has full knowledge about CSI and transmits quantized information about the CSI through limited feedback channel. Both of the transmitter and the receiver are equipped with a codebook that carries power loading vectors. The receiver decides the vector that has to be used and sends its index to the transmitter through feedback load, then the transmitter uses this vector to adapt transmission parameters. No feedback is needed in case when the maximum capacity is achieved where there is inactive power constraints. Otherwise, increasing the feedback load decreases the gap between the quantized CSI that is fed to the transmitter and the full CSI. Authors in [49] present power loading and subcarrier pairing in OFDM system that is based on limited feedback with considering different CSI's quantized levels. The feedback information depends on a codebook that is available at both of the transmitter and the receiver and is designed in an offline state. The constructed codebook - that depends on LIoyd algorithm in the vector quantization process - contains vectors for resource allocation. Full knowledge about CSI is assumed to be known perfectly at the receiver side. According to the CSI information, the most suitable resource allocation vector is chosen from the codebook and its index is fed to the transmitter through the limited feedback channel using a limited number of bits. To be able to decide the optimal codeword to have a maximized data rate in a specific region, a centroid condition is considered. Also, in a specific region, a neighbour rule is used to indicate the vectors that result in the nearest codeword to the optimal. When the receiver estimates the CSI, it searches in the codebook for the most suitable vector that gives the maximum data rate, then it sends its index to the transmitter through an error free feedback.

To reduce the feedback overhead, [50] introduces a strategy for limited feedback that is based on Grassmannian differential coding. The proposed strategy uses both of the Grassmannian structure and the temporal correlation of the wireless channel and it tracks the slow progress of the impulse response of the channel on the Grassmannian diverse. The receiver

estimates CSI and uses it along with the previous CSI to calculate the tangent vector. Then, the tangent vector is quantized and sent to the transmitter which uses it to reconstruct CSI. Also, the strategy is a function of the length of the channel, the channel mobility and the number of bits used for feedback from the receiver to the transmitter. The paper assumed a perfect channel estimation and feedback. Authors in [51] introduces a computationaly complex strategy for making the channel state information available at the transmitter through a channel norm feedback scheme and a channel phase codebook, which utilizes the correlation of the wireless channel in long-term perspective that changes in a slower manner than the instantaneous CSI. The representation of the channel is through a gain as well as phase representation schemes. The gain representation is derived from the channel norm and the phase representation depends on the channel phase codebook in which the matrix of the channel phase is quantized. This codebook is designed for several correlation conditions for the channel and is constructed offline using LIoyd algorithm. The channel perfect limited feedback bits contains the channel norm and the index of the corresponding channel phase in the codebook.

4.2 End-to-End Performance Evaluation

This section is concerned with end-to-end system performance evaluation and feedback techniques. Fig. 4.1 shows the block diagram of the end-to-end system. At the transmitter side, the input data is modulated, fed to OFDM Tx and transmitted through the forward channel. At the receiver side, the received signal is fed into OFDM Rx. After channel estimation process, the received signal is equalized. The estimated channel information is also sent in the limited feedback channel to be used for link adaptation. The Normalized Mean-Square Error (NMSE) between the actual and the feedback CSI over the N subcarriers and the K OFDM symbols is used as an evaluation criteria which is discribed as [45]:

$$NMSE = \frac{1}{KN} \frac{\sum_{i=0}^{K-1} \sum_{m=0}^{N-1} \left| H(m,i) - H_e'(m,i) \right|^2}{\sum_{i=0}^{K-1} \sum_{m=0}^{N-1} |H(m,i)|^2}. \tag{4.1}$$

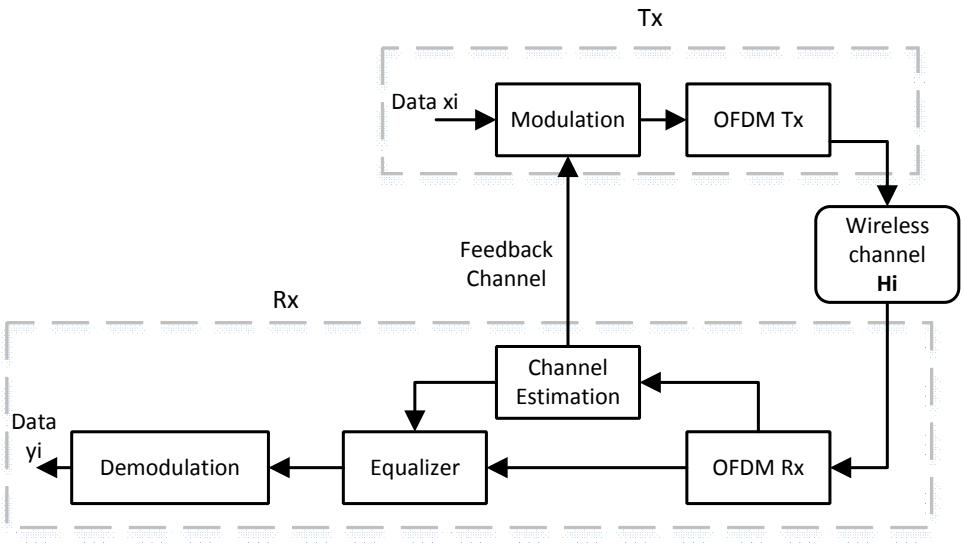

Figure 4.1. Block diagram for end-to-end system.

4.2.1 CSI Error Distribution:

In this part, the error between the actual and the feedback CSI is analysed. The OFDM signal is transmitted through a static 6-taps TU channel. At the receiver side, the frequency domain CSI is estimated using pilot subcarriers with $p_{\mathrm{f}} = 5$ subcarriers. Then the estimated CSI is quatized and fed back to the transmitter through a single path fading channel. Fig. 4.2 shows the variance of the distribution of the error between the actual and the feedback CSI. The variance is measured over a range of SNRs in the forward channel as well as the feedback channel. The figure shows that the error variance keeps decreasing by increasing the SNR either in forward or feedback channel. The decrease of the variance becomes very slow at high SNR because the effect of channel etimation errors and quantization errors becomes dominant.

Fig. 4.3 shows an approximation for the distribution of the error density at $SNR = 15dB$ in both of the forward and feedback channels. In the error distribution there are some outlayers caused by sever fading in the transmission channel, which were removed to be able to see the proper distribution fitting. The error between the actual and the feedback CSI

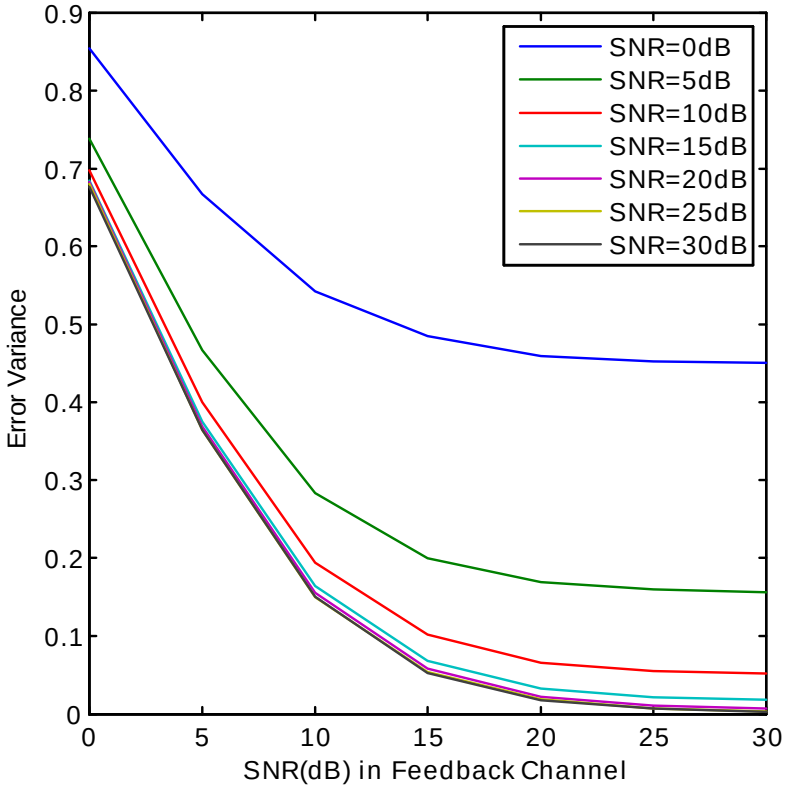

Figure 4.2. Error variance.

can be generally approximated by a gaussian distribution. The figure shows that in this case the gaussian distribution has a zero mean and 0.015 variance.

4.2.2 CSI Feedback Techniques:

The estimated CSI is conveyed to the transmitter side through feedback channel which is Modeled as a binary symmetric channel (BSC) with probability of error (p). Several feedback techniques are adopted in this section to send CSI back to the transmitter.

First Technique:

The approach of the first technique is to quantize the estimated coefficients of channel frequency response vector $\widehat{\mathbf{H}}_{\mathrm{P}} = [\widehat{H}_{\mathrm{P}}(1), \widehat{H}_{\mathrm{P}}(2), ...\widehat{H}_{\mathrm{P}}(N_{\mathrm{P}} - 1)] \in \mathbb{C}^{N_P \times 1}$at pilot subcarriers, and send it through feedback channel, to the transmitter where the interpolation takes place.

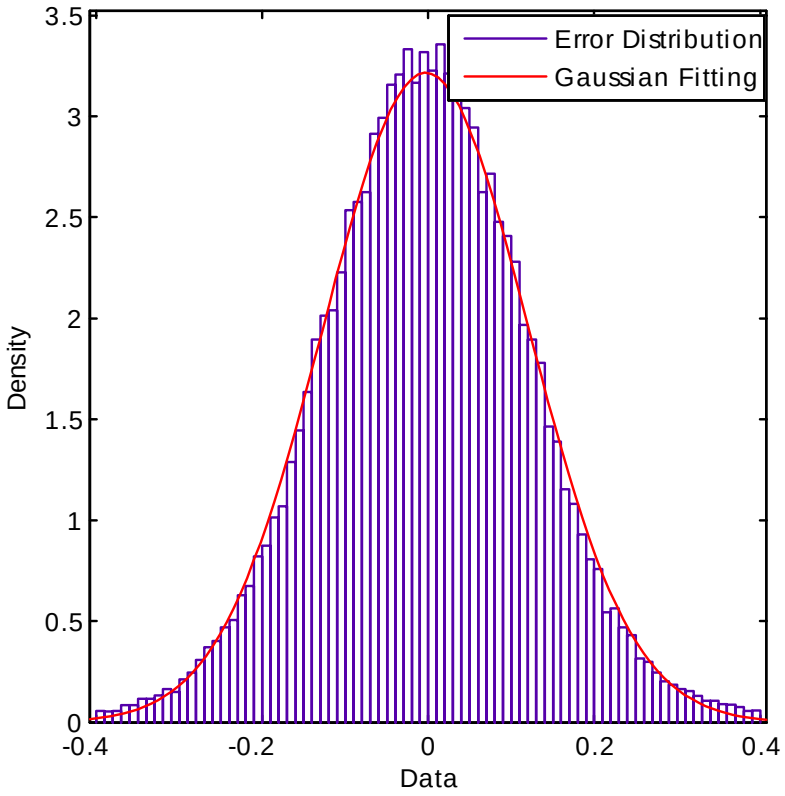

Figure 4.3. Distribution of the error between the actual and the feedback CSI.

Second Technique:

The second technique depends on the time domain vector of the CSI. The channel coefficients are estimated at pilot subcarriers and the interpolation takes place at the receiver side. Then the full estimated channel frequency response is converted into time domain through IFFT. The receiver quantizes the estimated time domain channel coefficient $\widehat{h}_m(t)$ at each sample, and sends the full quantized impulse response vector $\widetilde{\mathbf{h}}(t) = [\widetilde{h}_1(t),\ \widetilde{h}_2(t), ..., \widetilde{h}_{N-1}(t)]^T \in \mathbb{C}^{N\times 1}$ to the transmitter through feedback channel.

Third Technique (The Proposed CSI Feedback Technique using Truncated Channel Impulse Response):

In the proposed technique, the receiver feeds back the time-domain vector of the CSI instead of the corresponding frequency-domain in order to reduce the feedback overhead.

The length of the time domain vector is limitted to the length of the cyclic prefix N_{CP} . Since the number of cyclic prefix samples is chosen to be exceeding the the maximum multipath spread of the channel, the time domain vector of channel coefficients at samples with index above N_{CP} are assumed to be zero. Therefore, after the receiver estimates the frequency-domain vector of the CSI, it converts it to time domain using IFFT operation to get the time domain vector $\widehat{\mathbf{h}}(t) = [\widehat{h}_1(t),\ \widehat{h}_2(t), ..., \widehat{h}_N(t)]^T \in \mathbb{C}^{N\times 1}$, and then forces the elements with index above N_{CP} to be zero. After that, a vector of only N_{CP} elements ($\widehat{\mathbf{h}}_{\mathrm{CP}}(t) = [\widehat{h}_1(t),\ \widehat{h}_2(t), ..., \widehat{h}_{N_{CP}-1}(t)]^T \in \mathbb{C}^{N_{\mathrm{CP}}\times 1}$) is fed into the quantizer which can now act on a lower dimension vector to save the feedback overhead. Then, the quantized impulse response vector is $\widetilde{\mathbf{h}}_{\mathrm{CP}}(t) = [\widetilde{h}_1(t),\ \widetilde{h}_2(t), ..., \widetilde{h}_{N_{CP}-1}(t)]^T \in \mathbb{C}^{N_{\mathrm{CP}}\times 1}$. Consequently, at the transmitter, the received channel impulse response $\widetilde{\mathbf{h}}'_{\mathrm{CP}}(t)$ is padded with zeros to be of length N, then FFT operation is used to produce full channel frequency response to use it in link adaptation algorithm.

The factors determining the length of the feedback bits in the proposed time-domain approach are the length of the cyclic prefix N_{CP} and its ratio compared to N and the number of quantization bits b_{q}. The feedback overheadper OFDM symbol is $N_{\mathrm{CP}}b_{\mathrm{q}}$. In the simulation setup, $N_{\mathrm{CP}} = \frac{1}{8}N$, so $\frac{1}{8}Nb_{\mathrm{q}}$ bits is the length of feedback vector per OFDM symbol.

4.2.3 Number of Quantization Bits ($b_{\mathbf{q}}$):

This part evaluates the effect of the number of quantization bits on the NMSE between the perfect and the feedback channel frequency response. The channel response at each subcarrier is quantized using b_{q} bits, so CSI is quantized into $2^{b_{\mathrm{q}}}$ levels. In the first technique, the quantized channel ceofficients vector is $\widetilde{\mathbf{H}}_{\mathrm{P}} = \widehat{\mathbf{H}}_{\mathrm{P}} + \mathbf{q}_{\mathrm{P}}$, in the second technique, the quantized vector is $\widetilde{\mathbf{h}}(t) = \widehat{\mathbf{h}}(t) + \mathbf{q}_{\mathrm{N}}$, and in the third technique it is $\widetilde{\mathbf{h}}_{\mathrm{CP}}(t) = \widehat{\mathbf{h}}_{\mathrm{CP}}(t) + \mathbf{q}_{\mathrm{CP}}$. Where $\mathbf{q}_{\mathrm{P}}$, $\mathbf{q}_{\mathrm{N}}$ and $\mathbf{q}_{\mathrm{CP}}$ are quantization error vectors with dimentions $N_{\mathrm{P}} \times 1$, $N \times 1$ and $N_{\mathrm{CP}} \times 1$ respectively. Feedback overhead for the first technique is $N_{\mathrm{P}}(b_{\mathrm{q}})$ bits and it is $N(b_{\mathrm{q}})$ bits in the second one, while in the third technique the feedback overhead is $N_{\mathrm{CP}}(b_{\mathrm{q}})$ bits.

Increasing levels of quantization decreases quantization errors on the expense of feedback overhead.

The forward channel over which the evaluation is done is a static channel. The pilot separation used in channel estimation is 5 subcarriers. The probability of error in the feedback channel (p) is 10^{-4}, and the compared numbers of quantization bits (b_{q}) are 4, 5, 8, and 16 bits.

Fig. 4.4, Fig. 4.5 and Fig. 4.6 are related to the first, second and the third technique respectively. The figures show the NMSE between the actual and the feedback channel information as a function of SNR in the forward channel while each of the three techniques is used. In general, it is clear in the three figures that increasing the number of quantization bits has a major impact on improving the quality of the feedback CSI. It is shown that the NMSE decreases exponentialy with the increase of the number of bits. $b_{\mathrm{q}} = 8$ bits can be considered a sufficient number of quantization bits, as the improvement in the quality of the feedback CSI gained by using more quantization bits is not valuable where the source of error doesn't depend on the quantization errors any more. At high b_{q} values, quantization errors decrease and NMSE is dominated by imperfections caused by interpolation and errors in the feedback channel.

4.2.4 Probability of Error (p) in Feedback Channel:

The erroneous feedback channel is modeled as a Binary Symmetric Channel (BSC) with the error probability p. This part shows an evaluation of the effect of p in the feedback channel on the NMSE between the perfect and the feedback channel information. Note that the performance gain obtained from CSI feedback decreases as a result of increasing p. Pilot separation used in channel estimation is 5 subcarriers, the normalizaed doppler frequency in the forward channel is 0 and $b_{\mathrm{q}} = 16$. The results are taken over different SNR values for the forward channel.

Fig. 4.7, Fig. 4.8 and Fig. 4.9 show NMSE as a function of p for using each of the first, second and the third feedback technique respectively. It is shown clearly in the three figures

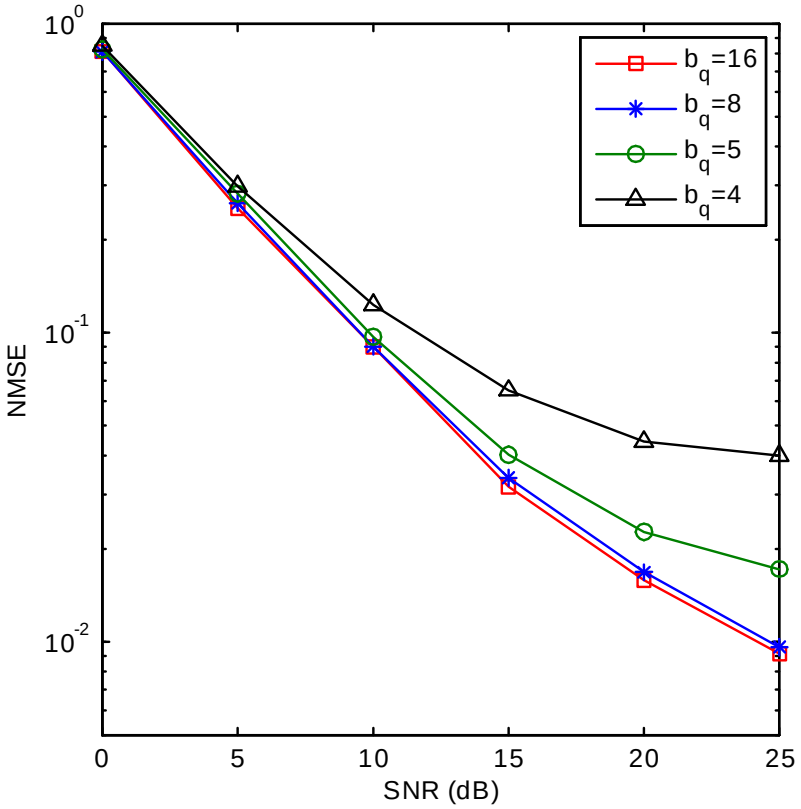

Figure 4.4. NMSE vs SNR (First feedback technique).

that NMSE decreases rapidly with the decrease of p values . In Fig. 4.7 for p less than 10^{-4}, the decay of NMSE becomes very slow and unsignificant. Therefore, $p = 10^{-4}$ represents the value where no improvement in the feedback quality is noticed beyond it. However, in figures (4.8) and (4.9) the decrease of NMSE for p less than 10^{-4} is still significant.

4.2.5 Comparison between CSI Feedback Techniques:

This part shows an evaluation of the differences in performance between the three feedback techniques in terms of the NMSE between the perfect and the feedback CSI, as a function of p in the feedback channel. SNR in the forward channel in which the techniques are evaluated is $20dB$. The number of quantization bits used at the receiver side before the feedback is 16 bits and the forward channel is a static channel.

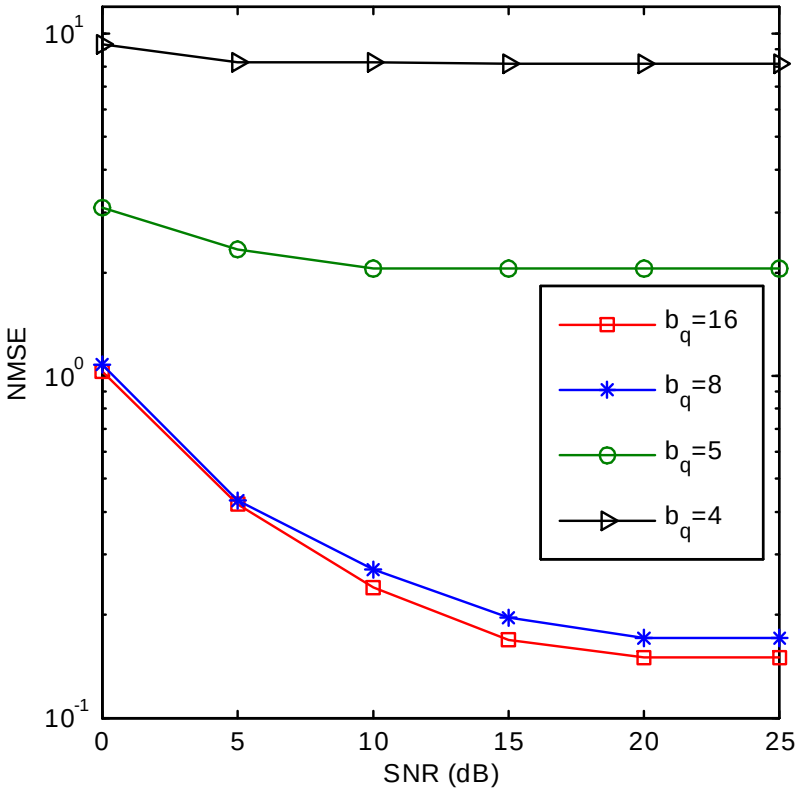

Figure 4.5. NMSE vs SNR (Second feedback technique).

Fig. 4.10 shows that the first technique -in which the frequency response of the channel at the pilot subcarriers is feedback to the transmitter- performs better than both of the other techniques at high p values, because using FFT to convert from time to frequency domain in the second and the third technique, makes them more sensitive to errors and causes an increase in the error variance between the perfect and the feedback CSI. In the second technique, after applying FFT to the received CSI in time domain $\mathbf{h}'(t)$, the frequency domain CSI is described as:

$$H'(k) = \sum_{n=0}^{N-1} h'(n) e^{-j2\pi kn/N} \tag{4.2}$$

where $\mathbf{h}^{'} = \mathbf{h} + e^t$, and $\mathbf{H}' = \mathbf{H} + e^f$, where variance of the error e^t is σ_t^2 and the variance of the error e^f (which is the output of FFT) is $\sigma_f^2 = N\sigma_t^2$.

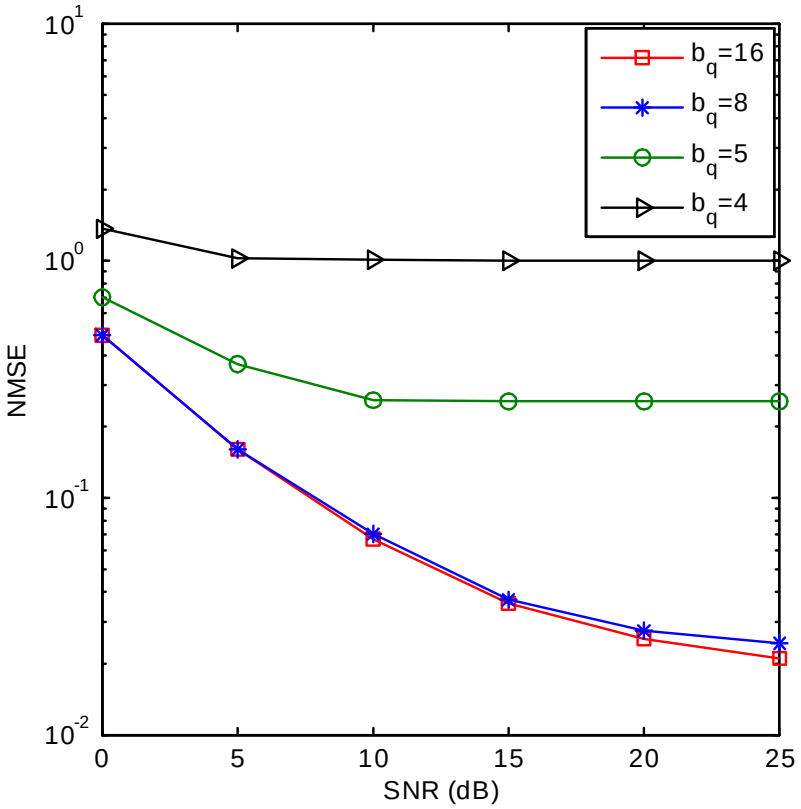

Figure 4.6. NMSE vs SNR (Third feedback technique).

When the CSI vector is quantized and transmitted through the erroneous feedback channel, error bits can take any position in the quatized vectors. So, if the error bit is in the position of the Most significant bit (MSB) or near to it, this makes that quantized CSI values jump to a quantization level that is far from its actual one. If the vector of the CSI is in time domain, such errors may propagate to the whole CSI vector and be enlarged when the vector is transformed to frequency domain through FFT operation. This makes the time-domain feedback approaches (second and third techniques) in a need to small values of p to perform better that the frequency-domain feedback technique.

Also, it is shown in the figure that the quality of the received CSI using the third technique outweigh the quality gained by using the second technique. That is because, in the second technique, the impulse response of the channel on the N samples is feedback to the

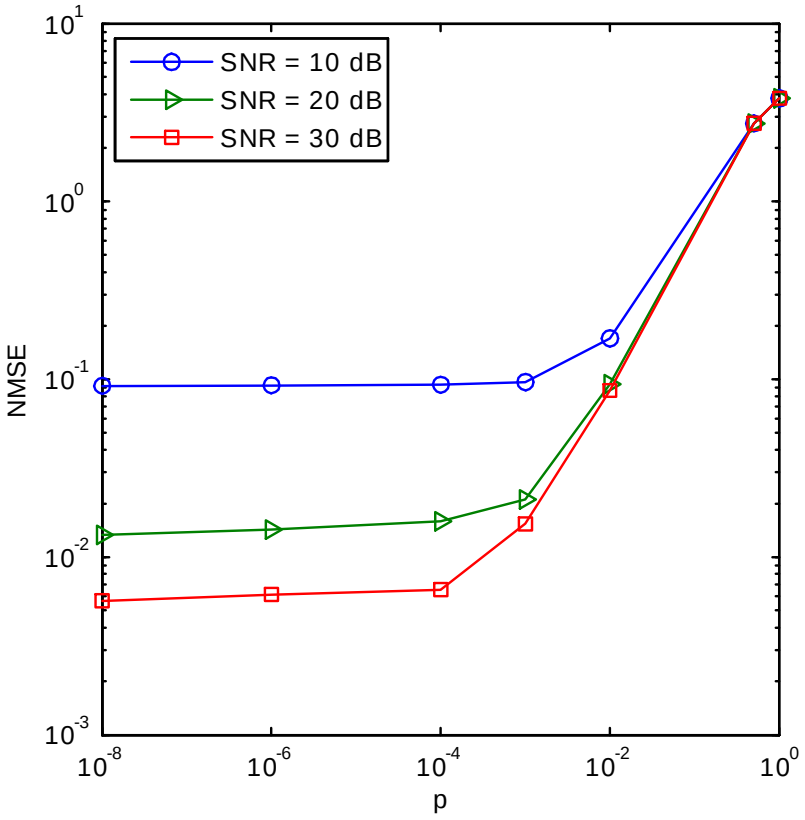

Figure 4.7. NMSE vs p (First feedback technique).

transmitter, while in the third technique, the channel impulse response only at N_{CP} samples is feedback to the transmitter, where the errors in feedback is only limitted to N_{CP} samples, this is due to the use of zero forcing in time domain vector elements with index above N_{CP} which acts like a filtering process to CSI ceofficients to make it closer to the actual values. Actually, CSI ceofficients on $N - N_{\text{CP}}$ samples are nulled due to the assumption that the number of cyclic prefix samples is chosen to exceed the the maximum multipath spread of the channel. So, after converting to the frequency domain, the error propagation in the N subcarriers will be much smaller than the case of the second technique.

Fig. 4.10 shows that the Third Technique performs better than the other two techniques at low to moderate values of p. This is due to the use of zero forcing to the time-domain

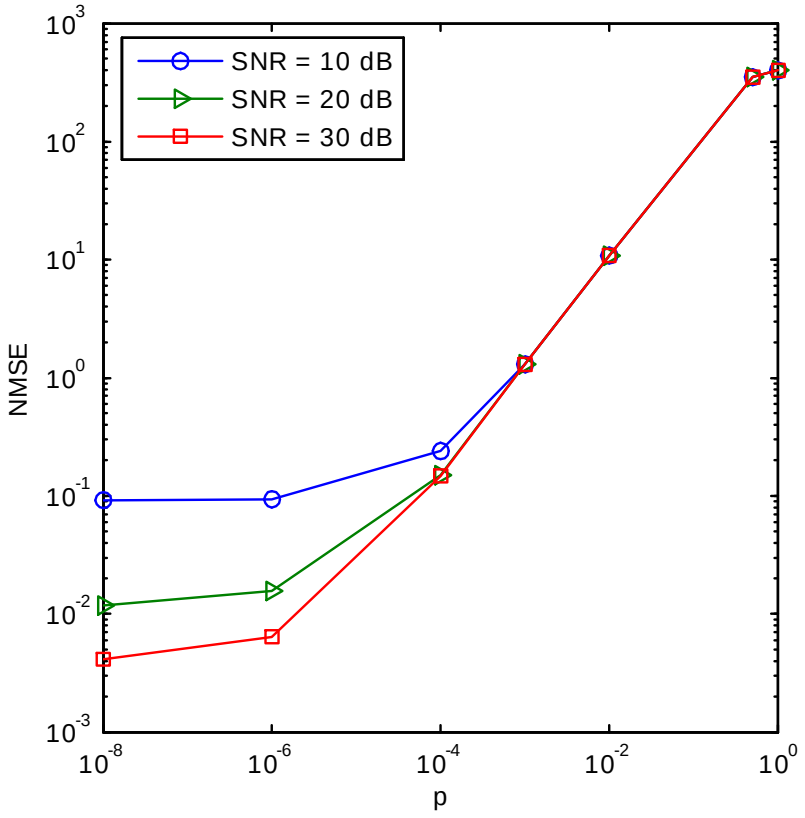

Figure 4.8. NMSE vs p (Second feedback technique).

CSI at $N - N_{\text{CP}}$ samples which has the ability to filter the CSI vector to improve its quality as it makes it closer to the actual one.

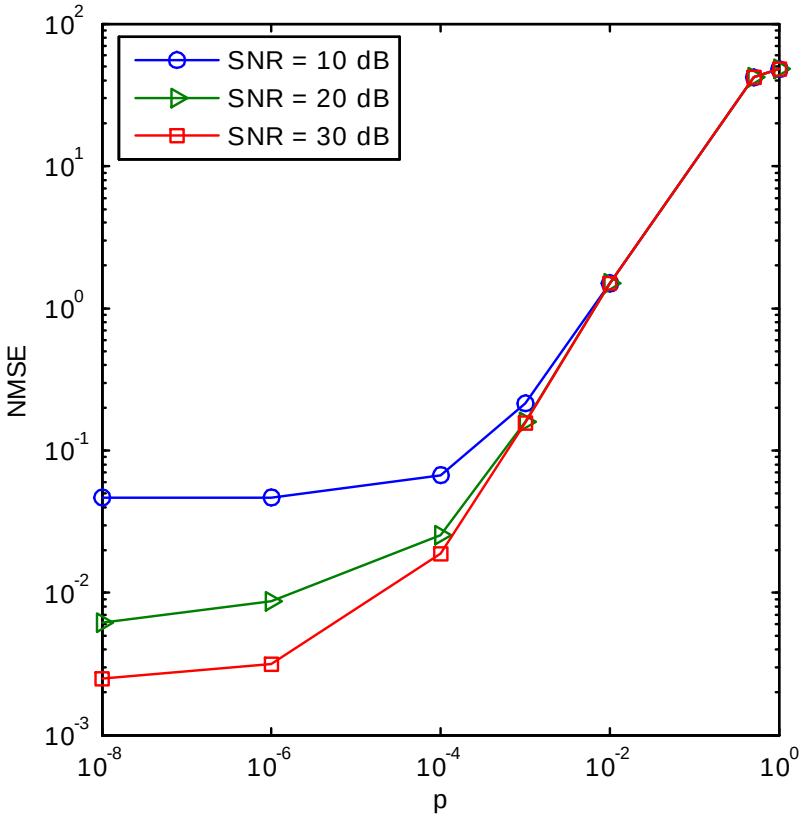

Figure 4.9. NMSE vs p (Third feedback technique).

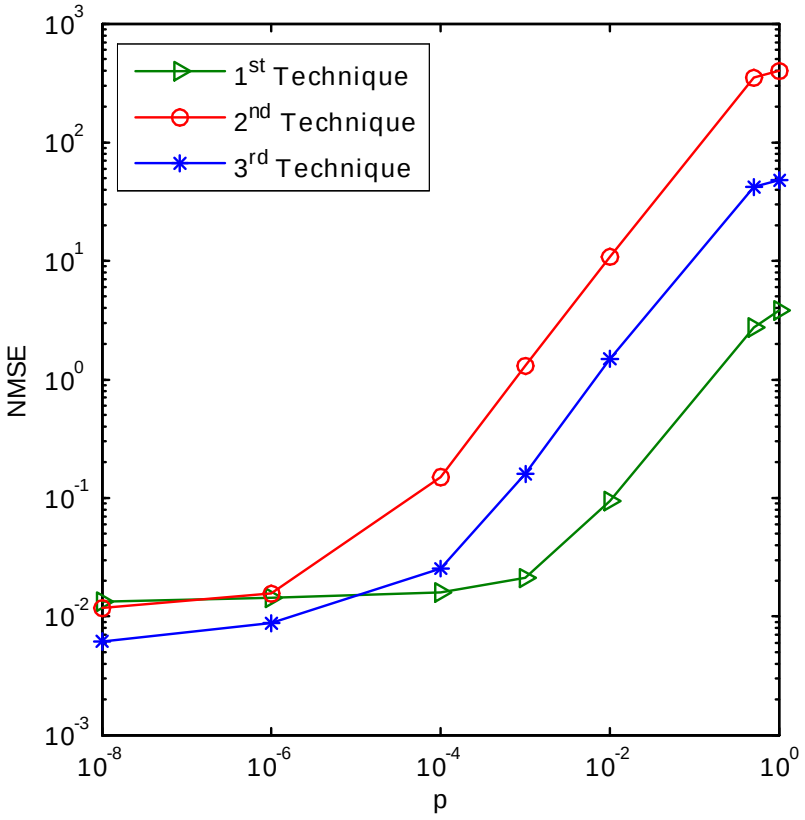

Figure 4.10. Comparison between the three feedback techniques at SNR=30dB.

CHAPTER 5

LINK ADAPTATION USING TRUNCATED CHANNEL IMPULSE RESPONSE FEEDBACK

5.1 Introduction

Achieving a reliable adaptive wireless communication system depends mainly on the availability of the channel state information (CSI) at the transmitter side which is obtained through feedback from the receiver side to the transmitter side through a limited feedback channel. Limmitation and imperfections like error and delay in the feedback channel can severely degrade the reliability of CSI feedback. Therefore, it has been recently an attractive topic for researchers.

Authors in [39] introduced an adaptive OFDM communication system where the transmitter receives only one bit per subcarrier through feedback. That is done through dividing all CSI conditions into two groups only. The system parameters are designed according to IS-136 standard and channel estimation is assumed to be perfect. The adaptive techniques used in this system are: adaptive subcarrier selection (ASCS), adaptive power allocation (APA) and adaptive modulation selection (AMS). BER is the only criterion used to evaluate the techniques performance. Limitation of the limited feedback channel (like errors and delay) and their effects on the performance of the used link adaptation techniques are studied and evaluated. Considering the effect of different delays is done through considering a range of correlation coefficient values. A critical correlation coefficient value is defined, below whom the adaptive techniques give worse performance than that in the non-adaptive system. Also, evaluating the bit error rate on high values of SNR shows that APA technique is less robust

than AMS towards delays in feedback channel. However, AMS is worse than non-adaptive modulation in high erroneous feedback channel. Also, when the feedback channel becomes unreliable, it is better to uniformly distribute power among subcarriers.

[52] shows a study for link adaptation algorithm that depends on the feedback of a defined codebook index. The feedback channel is assumed to be outdated and has finite rate. Authors in [52] derived expressions for the probability density function of the SNR of the output of the receiver as well as closed form expressions for the moment generating function and these expressions include the effect of the delayed and limited-rate feedback channel. The analysis of the SER for different delays in feedback -at a normalized Doppler shift = 0.01- shows that in general, the SER becomes worse by the increase of the delay compared to no-delay situations, it also shows that along the increase in the delay, the SER degrades first, till it reaches a stage where it fluctuates as a function of the feedback delay as well as the autocorrelation function of the fading channel, but no improvement techniques are provided. Erroneous channel estimation effects are not considered in this paper.

Work in [53] shows a study of beam forming in MIMO communication system through sending quantized channel state information (CSI) in limited feedback channel. Considering the channel estimation errors is absent in this paper. On the other hand, outdated feedback channel is studied through analysis that includes the rate of the output of the CSI quantizer, the bit rate of the limited feedback channel and the effect of the feedback delay on the throughput of the communication system. The limited feedback is studied in this paper over temporally correlated channels. The generation of the simulation results depends on Rayleigh fading and Clarke's fading channel models. Results show that when the Doppler shift increases, the bit rate of CSI feedback increases in a linear relation. Results also show that the feedback throughput decreases exponentially with the feedback delay. A design example discusses the effect of Doppler shift on the tolerable feedback delay which is represented through an inverse relation.

In [34], authors present a study for the effect of the delay in feedback channel with the existence of uncoordinated other cell interference in cellular system. The feedback delay considered in this paper is mainly a result of signal processing, propagation delay as well

as channel access protocols, and the realistic values which are used in analysis are 4 and 6 ms. Channel estimation depends on pilots and it is assumed to be perfect. Goodput metric is used in analysis and it shows an upper limit of the feedback communication system in the presence of delayed feedback. As delay in the limited feedback channel increases, the goodput gained decreases doubly exponentially. Some results in this paper show that smaller time correlation in the channel results in faster goodput decay with feedback delay.

[54] proposed an approach to reduce the requirements of the feedback and to increase the resolution and the reliability of CSI feedback to the base station in multicell systems. The proposed approach takes advantage of temporal correlation in the communication channels. This work takes into consideration the effects of feedback delay (assumed to be 2 frame durations which is equal to 2ms) on the reliability of CSI feedback at the base stations. Given a codebook, the most suitable codewords are chosen for adaptation. The proposed approach shows that higher complexity can be the cost of improving the performance in the presence of feedback delay.

In [55], authors study the design of pilot symbol assisted modulation (PSAM) with the use of feedback channel. A time varying channel is considered as well as an outdated limited feedback channel. In this work link adaptation is done through power adaptation strategy in order to optimize the capacity. The analysis considered high and low mobile fading channel and it is showed that at low doppler frequencies, higher information rate is guaranteed and it decreases with the increase of the feedback delay, but in all cases its performance is better than the systems with no feedback links. On the other hand, it is proved that in fast fading channels, the gains of the power adaptation schemes are dissipated even with low feedback delay.

5.2 Frequency-Domain Feedback Technique:

Mobile WiMax parameters are adopted in OFDM system. In this section, CSI is etimated at the receiver side using pilot-aided channel estimation. The feedback technique is the first technique explained in chapter 4. Its approach is to quantize the estimated coefficients

of channel frequency response vector $\widehat{\mathbf{H}}_{\mathrm{P}} \in \mathbb{C}^{N_P \times 1}$at pilot subcarriers, and send it through feedback channel to the transmitter where the interpolation takes place. The pilot separation (P_{f}) that is used in simulation is 5 subcarriers and the number of bits used in quantization (b_{q}) of the CSI is 8 bits. The forward channel is a frequency selective channel, where 6-taps Urban channel model is adopted.

5.2.1 Erroneous Feedback

In this part, the effect of errors in the feedback channel on the introduced adaptive modulation algorithm is evaluated. The forward channel is a static channel and the erroneous feedback channel is modeled as a dinary symetric channel (BSC) with probability of error p.

Fig. 5.1 shows the average bit error rate ($\overline{BER}$) as a function of the probability of error in feedback channel (p) over different values of $\overline{\gamma}$. It is shown in the figure that when the actual CSI is used in a daptation, $\overline{BER}$ is less than or equal to BER_T. However, when the feedback channel is an imperfect channel, it means that the transmitter received erroneous information about CSI, so $\overline{BER}$ becomes larger than BER_T. Even when p is small like the case when $p = 10^{-3}$. For $p = 0$, the average bit error rate is still higher than BER_T because of errors caused by interpolation used to have the full estimated CSI as well as the errors caused by quantization process where the actual values of the CSI are approximated.

Fig. 5.2 clarifies the idea by showing the actual CSI compared with the feedback CSI at $p = 10^{-3}$. The figure shows snapshots of the actual channel frequency response and the feedback at average forward SNR $= 0dB$ and $20dB$. It is clear from the two figures that at low to moderate $\overline{\gamma}$ values, the channel estimation is not perfect enough and errors caused by quantization degrade the quality of the feedback CSI which can affect the quality of the adaptive modulation algorithm.

Fig. 5.3 is a snapshot of the feedback CSI at $p = \{10^{-3}, 10^{-2}, 10^{-1}\}$ in the feedback channel, evaluated at $\overline{\gamma} = 30dB$ in the forward channel. The actual CSI is also shown in the figure for the seek of comparison. It is clearly shown that even with high $\overline{\gamma}$ values, the quality

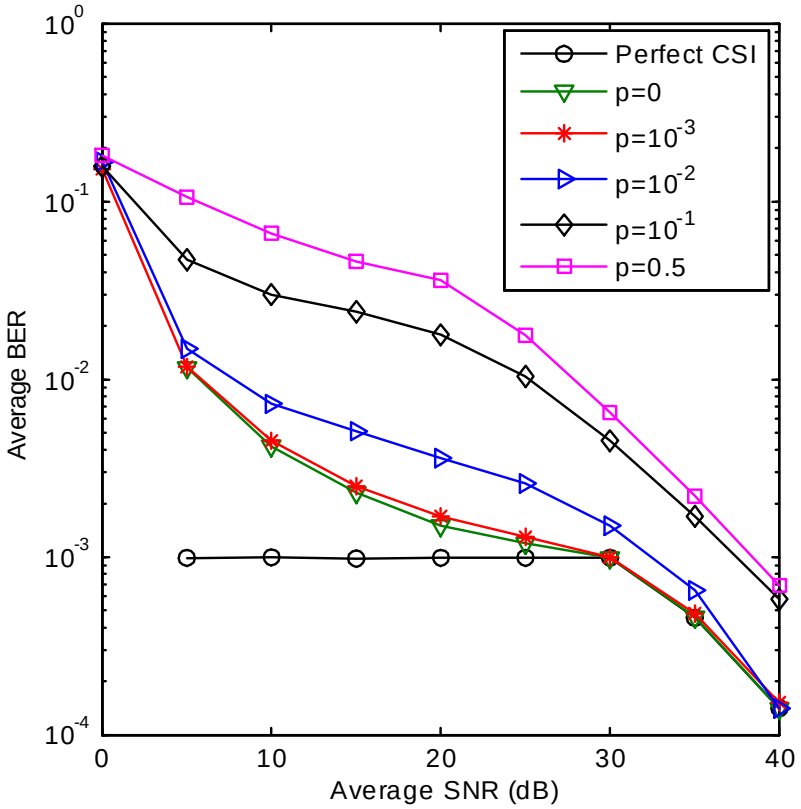

Figure 5.1. BER of adaptive system with erroneous feedback.

of the feedback CSI degrades with the increase of the probability of error in the feedback channel which explains the degragation in $\overline{BER}$ shown in Fig. 5.1.

5.2.2 Delayed Feedback

In this part, the adaptive modulation algorithm behaviour is evaluated under the effect of imperfections in the the feedback channel due to delay. The evaluation considers the effect of delay over different mobility conditions.

Fig. 5.4 shows how the average BER is affected by delay in terms of OFDM symbols with different channel doppler shift values as F_{d} range is from 0.004 to 0.12. It appears in the figure that changing F_{d} controls how fast the change in the average BER occurs. As F_{d} increases,

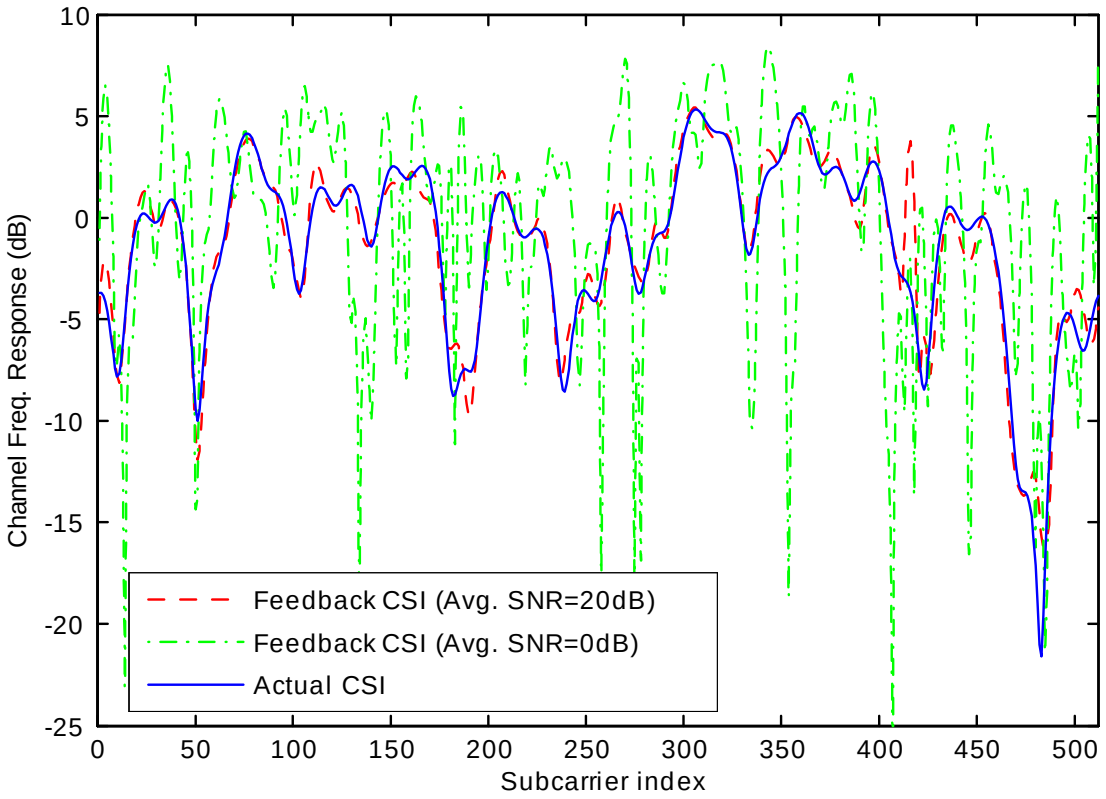

Figure 5.2. Snapshots of the frequency response of the actual channel and the feedback channel at $p = 10^{-3}$.

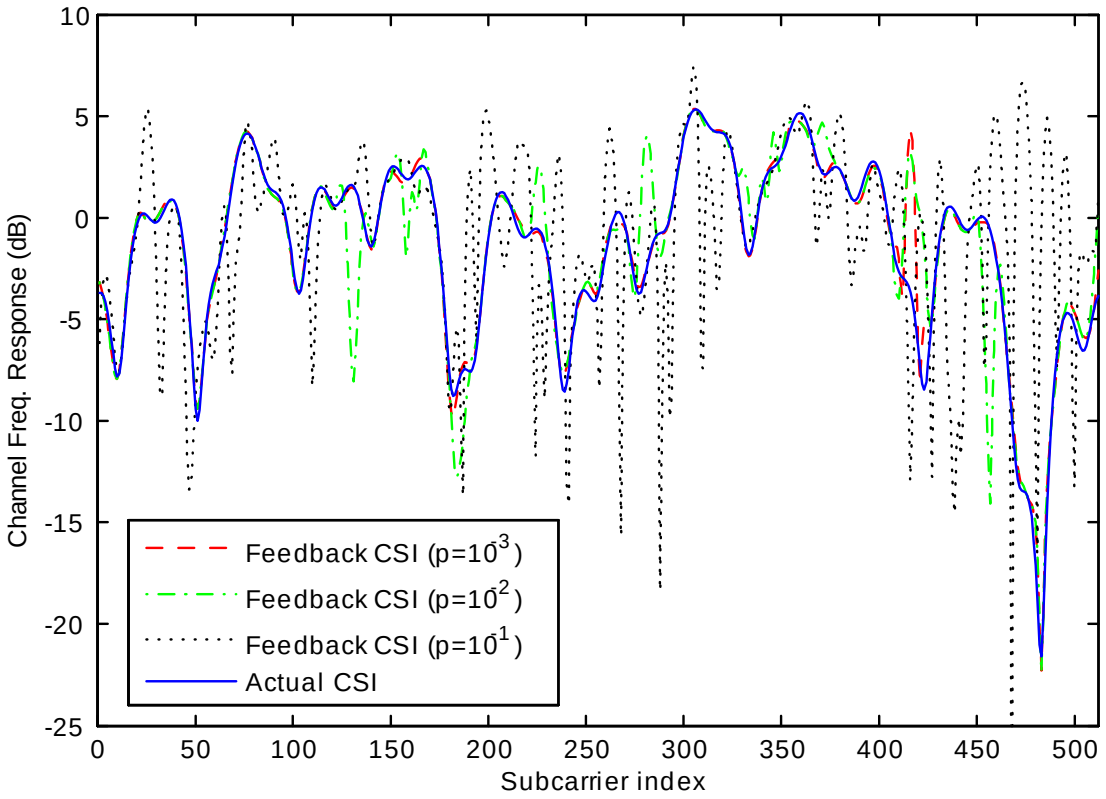

Figure 5.3. Snapshots of the frequency response of the actual channel and the feedback channel at average SNR $30dB$ in the forward channel.

the increase in the average BER values becomes faster until it reaches its maximum for each F_d value. This is because by increasing mobility, the changes of the channel gains over time becomes more significant so that, delay can mislead the bit allocation over subcarriers. The next two figures explain the changes in the worst BER values with diffirent normalized doppler frequency values.

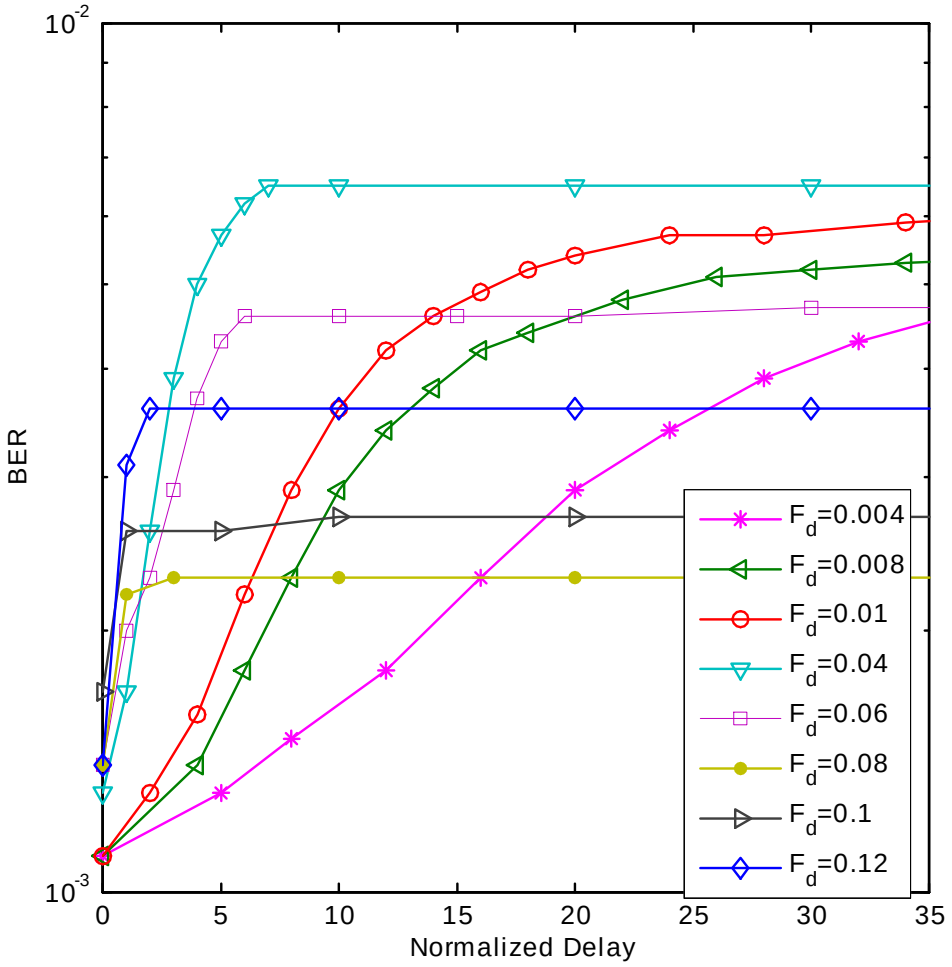

Figure 5.4. Average BER vs delay in OFDM symbols and average SNR = 30dB.

Figures 5.5 and 5.6 show evaluation of the impact of increasing the channel mobility on the average throughput as well as the average BER at a fixed delay of 10 OFDM symbols. Figure (5.5) shows a slow decrease in the number of bits transmitted per subcarrier per

OFDM symbol, with the increase of the normalized doppler value at average SNR=20dB . As a result, in Fig. 5.6, the average BER vs F_{d} increases rapidly at the begining because the channel interference due to doppler increases by increasing mobility, then $\overline{BER}$ becomes nearly constant as it reached its worst value.

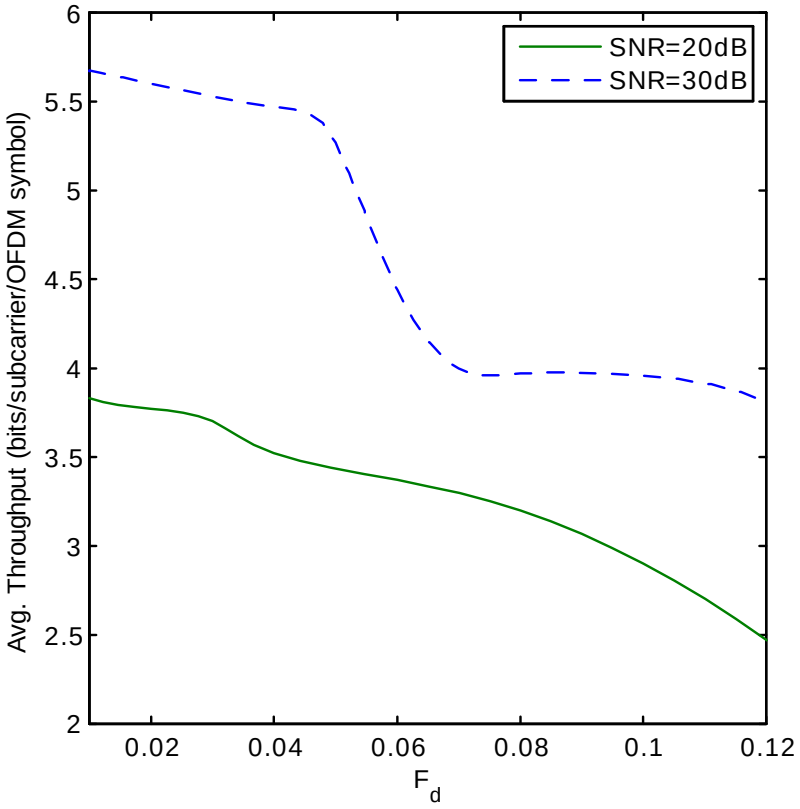

Figure 5.5. Average throughput vs $\mathrm{F_d}$.

In Fig. 5.5, at average SNR value of 30dB, the average throughput decreases in a very slow manner. Therefore, the Average BER increases as in Fig. 5.6 as discussed before. Also, it is shown in both figures that when the average throughput decreases rapidly, a noticeable improvement in the average BER occurs with the increase of F_{d}, because lower order of modulation scheme is used. After this improvement, Fig. 5.6 shows that the average BER increases again due to the slow manner of decreasing in the average throughput that is followed by the adaptation algorithm with the increase in the channel mobility. This

behaviour is a result of using nearly the same modulation order while the channel interference becomes more sever with the increase of F_{d}.

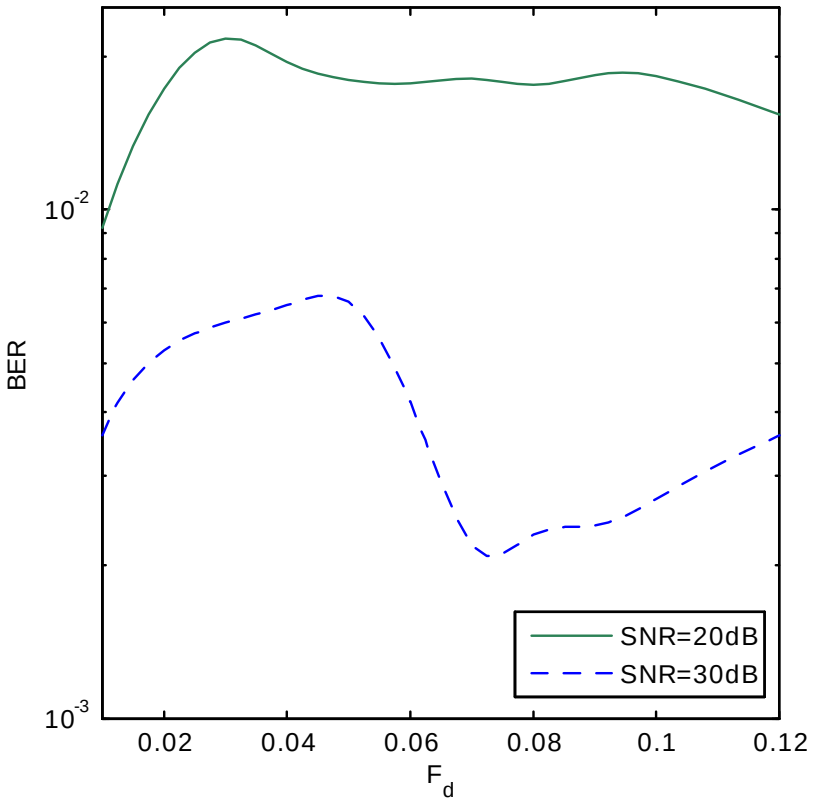

Figure 5.6. Average BER vs $\mathrm{F_d}$ at delay of 10 OFDM symbols.

5.3 Time-Domain Feedback Technique:

This part shows an evaluation to the performance of the adaptive modulation algorithm using the proposed truncated time domain feedback which is the third feedback technique explained in chapter 3. The receiver feeds back the time-domain vector of the CSI instead of the corresponding frequency-domain vector in order to reduce the feedback overhead. The length of the time domain vector is limited to the length of the cyclic prefix N_{CP} .

The factors determining the length of the feedback bits in the time-domain approach are the length of the cyclic prefix N_{CP} and its ration compared to N and the number of quantization bits b_{q}. The feedback overhear per OFDM symbol is $N_{\mathrm{CP}} b_{\mathrm{q}}$. In the simulation setup, $N_{\mathrm{CP}} = \frac{1}{8}N$, so $\frac{1}{8}Nb_{\mathrm{q}}$ bits is the length of feedback vector per OFDM symbol.

BER performance is examined using various values of p (the probability of error in the feedback channel), range of delay in terms of OFDM symbols and b_{q} (number of quantization bits).

5.3.1 Erroneous Feedback

Fig. 5.7 and 5.8 show the Average BER vs the Average SNR in the forward channel, tested over several values of p in the feedback link and the forward channel is assumed to be a static channel. The pilot separation used in channel estimation is 5 subcarriers. In Fig. 5.7 BER is evaluated using $b_{\mathrm{q}} = 8$ bits, by which the total feedback overhead becomes $\frac{1}{8}Nb_{\mathrm{q}} = \frac{1}{8}N \times 8 = N$ bits per OFDM symbol which means that only 1 bit per subcarrier is fedback to the transmitter. A clear improvement in the quality of the data occurs, as the BER decreases by decreasing the value of p, appears in Fig. 5.7. The figure also shows BER of the signal when the modulation is adapted using the actual CSI and how it differs from the BER when the adaptation is done using the estimated and quantized CSI at $p = 0$. This difference appears as a result of the loss due to the quantization process and due to the interpolation used to get CSI values in channel estimation as some values of the actual CSI are approximated.

Fig. 5.8 shows BER evaluation using $b_{\mathrm{q}} = 4$ bits, by which the total feedback overhead becomes $\frac{1}{8}Nb_{\mathrm{q}} = \frac{1}{8}N \times 4 = N/2$ bits per OFDM symbol which means that only 1 bit every 2 subcarriers is fed back to the transmitter. When comparing this figure to Fig. 5.7 it is found that a significat degradation in the signal quality appears when b_{q} is decreased to 4. This result is due to the high selectivity of the forward channel which requires a relatively big number of quantization bits to be able to present CSI values accurately.

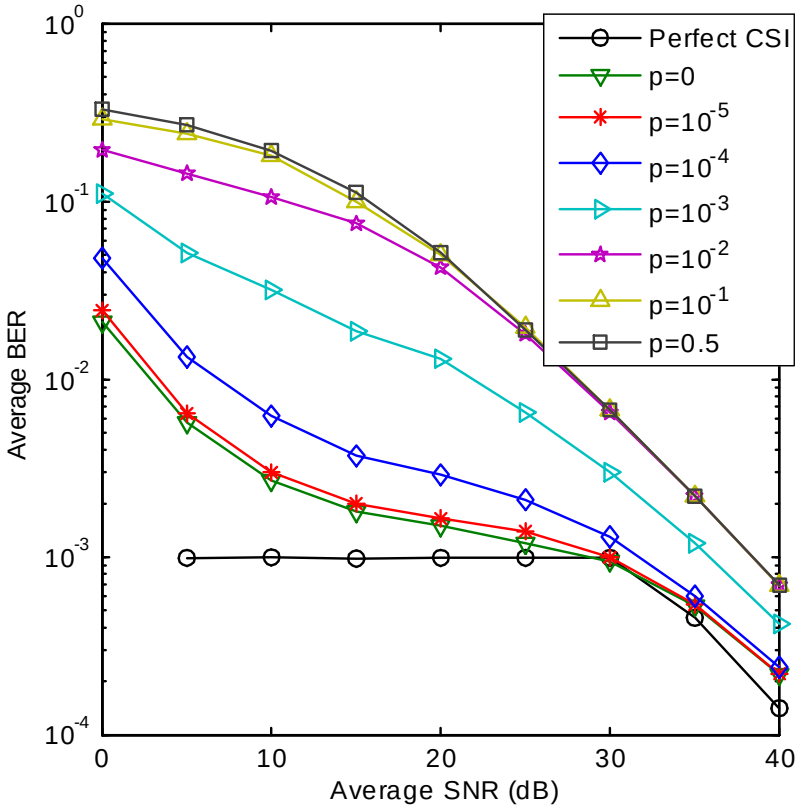

Figure 5.7. Average BER vs average SNR using time-domain feedback at b_{q}=8 bits.

5.3.2 Delayed Feedback:

An evaluation of the BER vs feedback delay in terms of OFDM symbols is shown in Fig. 5.9 over Average SNR values $10, 20$ and $30dB$ at F_{d}=0.1. The figure shows that as the feedback delay increases, the Average BER at first degrades, but then fluctuates with the increase of delay. These fluctuations fit the behavior of the fading channel autocorrelation function ρ_d as a function of delay (section 3.3).

Fig. 5.10 shows the average BER vs feedback Normalized delay with respect to OFDM symbols, over different F_{d} values. It is clear in the figure that as the delay increases, the BER generally becomes significantly worse with respect to all F_{d} values. On the other hand, the amount of degradation in BER with the increase in the delay is determined by F_{d},

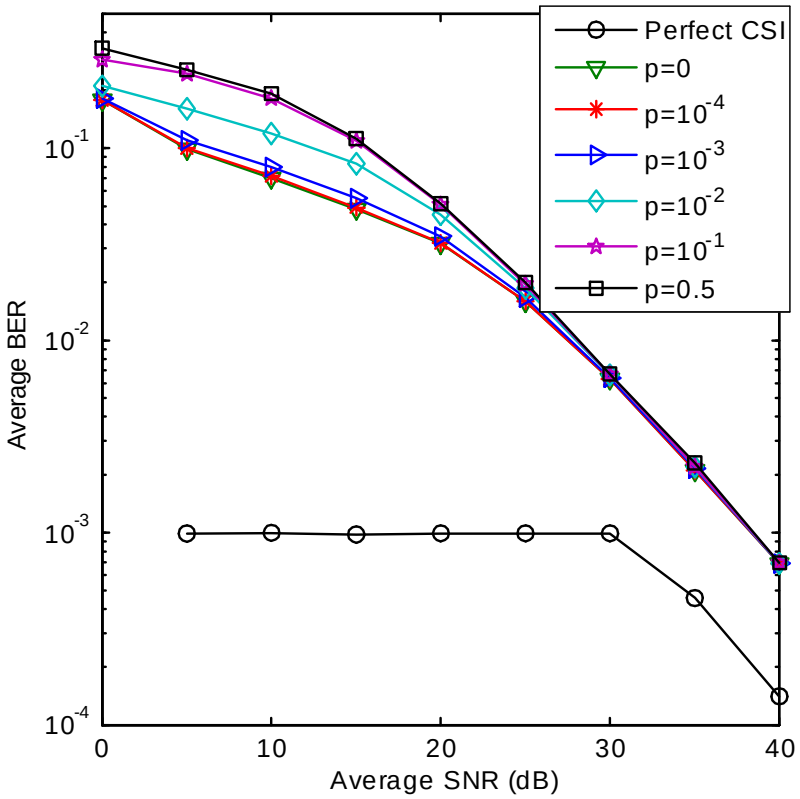

Figure 5.8. Average BER vs average SNR using time-domain feedback at b_q=4 bits.

as the speed of the increase in the BER values increases with the increase of the doppler shift. Since the changes of the channel gains over time as well as interference become more significant with increase of F_d, any small delay can cause a mismatch in the bit allocation over subcarriers which affects the signal quality significantly.

Fig. 5.11 shows the behaviour of the Average BER as a function of F_d. The simulation results of the BER are taken at a delay of 5 OFDM symbols. The fluctuations that appear in the BER values with respect to the increase in mobility can be a response to the throughput behaviour of the bit allocation algorithm that is shown in Fig. 5.12. It is observed in the two figures that having a constant throughput or a slow decreasing throughput with the increase of F_d, degrades the BER behaviour because with the increase in mobility, the channel interference becomes worse. Also, it is noticed that an improvement in the BER

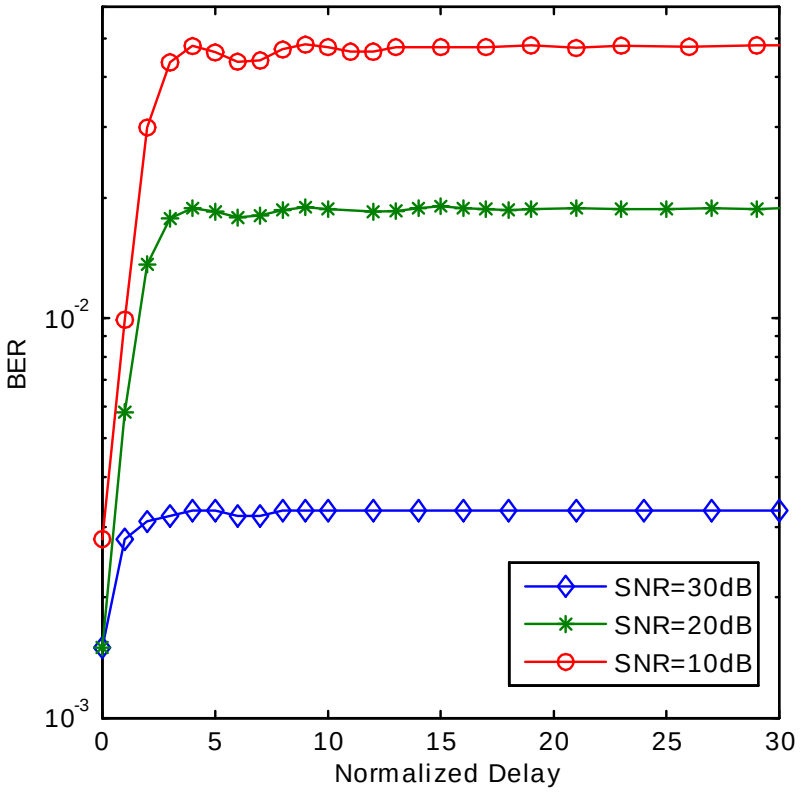

Figure 5.9. Average BER vs delay at F_{d} =0.1.

happens as a response to a significant decrease in the throughput of the adaptation algorithm, because a lower order of modulation scheme is used.

5.4 Comparison between Time-domain Feedback and other Techniques

Fig. 5.13 compares between adaptive modulation using CSI frequency-domain feedback (FDF) and using the proposed CSI limited time-domain feedback (TDF) and both are evaluated with $b_{\mathrm{q}} = 8$ bits and $F_{\mathrm{d}} = 0$. The comparison is based on the average BER performance vs the Average SNR. It is shown in the figure that time-domain feedback performs better than frequency domain at low to moderate SNR values, and they perform approximately

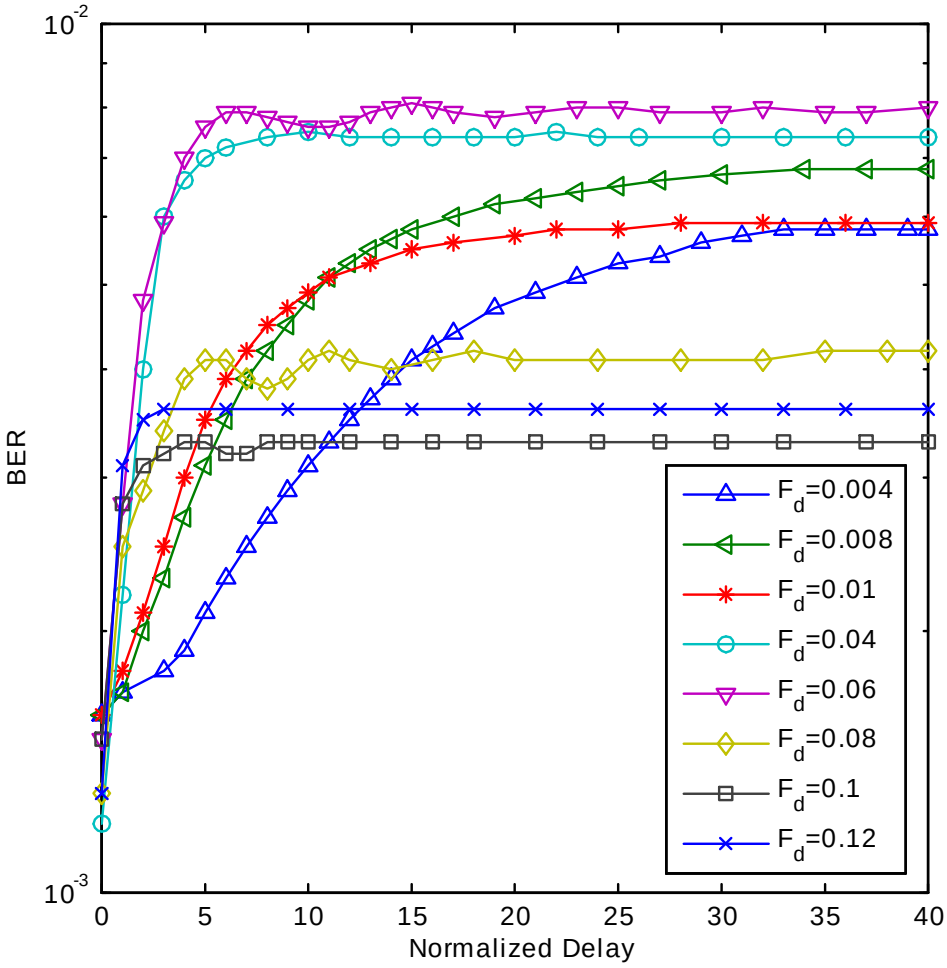

Figure 5.10. Average BER vs delay in OFDM symbols and average SNR = 30dB using TDF.

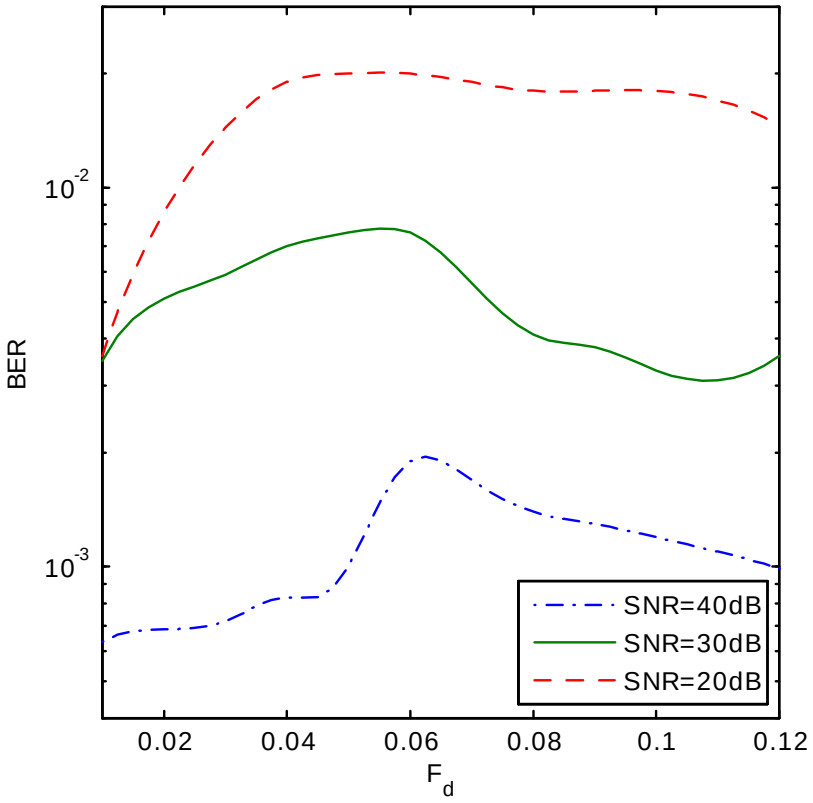

Figure 5.11. Average BER vs F_d at delay of 5 OFDM symbols.

the same at high SNR values. This is due to the use of zero forcing in time domain vector elements with index above N_{CP} which acts like a filtering process to CSI ceofficients to make it closer to the actual values.

Fig. 5.14 and Fig. 5.15 compare the proposed Time-domain feedback technique (TDF) to one-bit feedback (OBF) technique proposed in [39]. The figures have simulation results for the adaptive modulation technique that adapts between QPSK, 16-QAM and 64-QAM for each subcarrier according to average BER constraints as explained before. The time-domain feedback technique uses N bits feedback overhead per OFDM symbol. This is compared to the one bit feedback technique which also uses N bits feedback overhead per OFDM symbol [39] but it can choose between nulling the subcarrier or modulating it using M-QAM, also according to the same BER constraints.

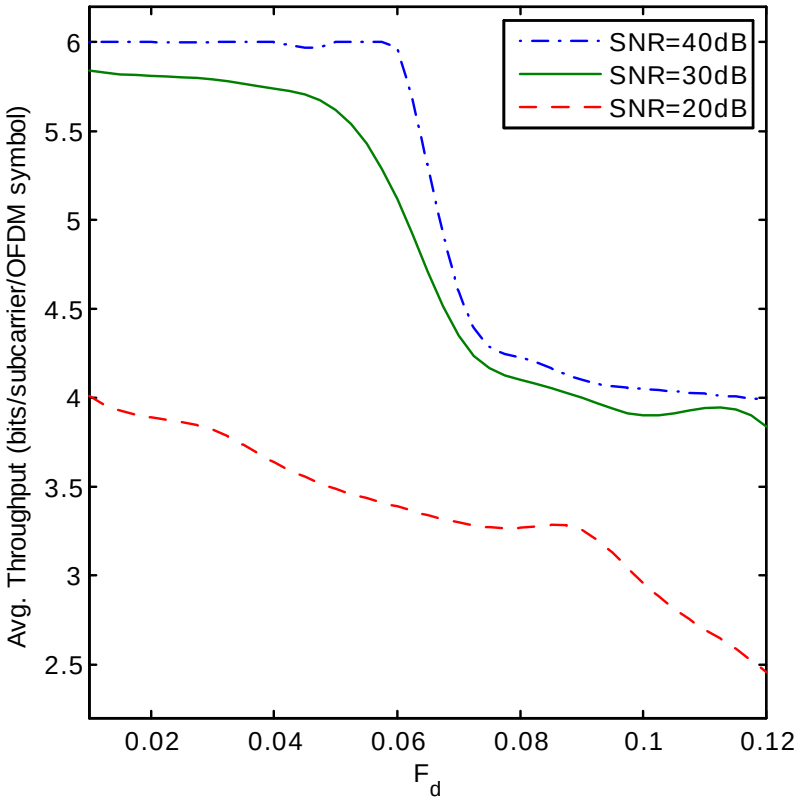

Figure 5.12. Average throughput vs F_d.

Fig. 5.14 shows that at first the time domain feedback technique outperforms the one bit technique. Then, OBF which chooses between null and QPSK for each subcarrier performs better, because more throughput is adopted in the adaptive modulation algorithm that uses TDF .

To have a more clear comparison, Fig. 5.15 shows the simulation results of the comparison between the two techniques using the average goodput. Average Goodput is defined as the average number of bits received correctly. It can be seen that the proposed time domain feedback gives more freedom and flexibility to link adaptation, as it gives to the transmitter enough information about the channel. So, the transmitter in this case can adapt between a number of modulation schemes that is bigger than the number adopted by the one-bit feedback technique. Only two modulation schemes can be used when the OBF technique is

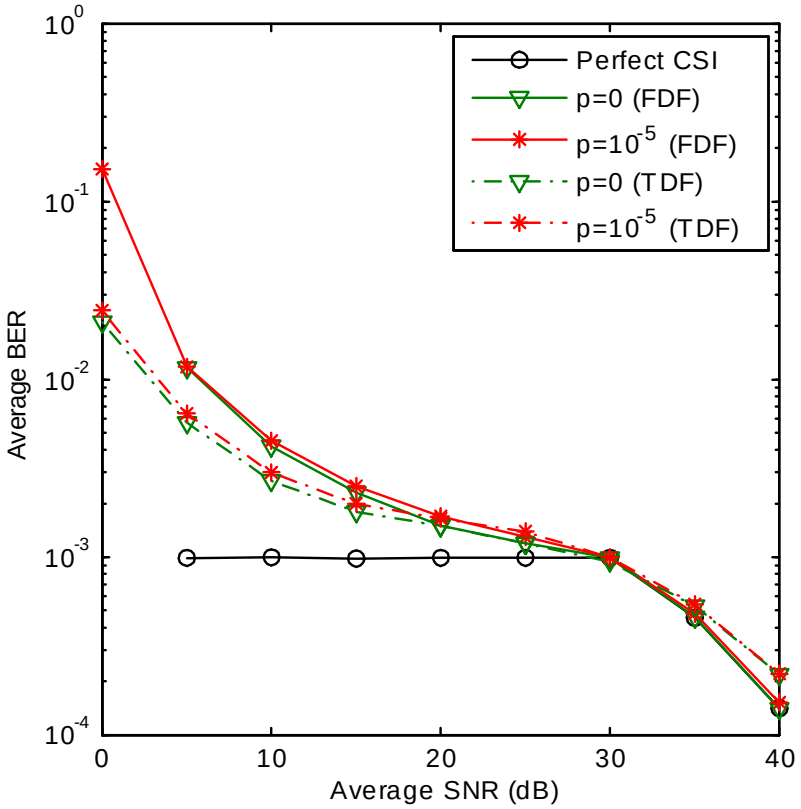

Figure 5.13. Comparison between frequency domain feedback and time domain feedback at $b_q = 8$ bits.

used because it gives very limited information about CSI and divides all possible channel gains into two levels only. That's why the Goodput of the adaptive modulation using TDF is always higher than that of the adaptation using OBF technique.

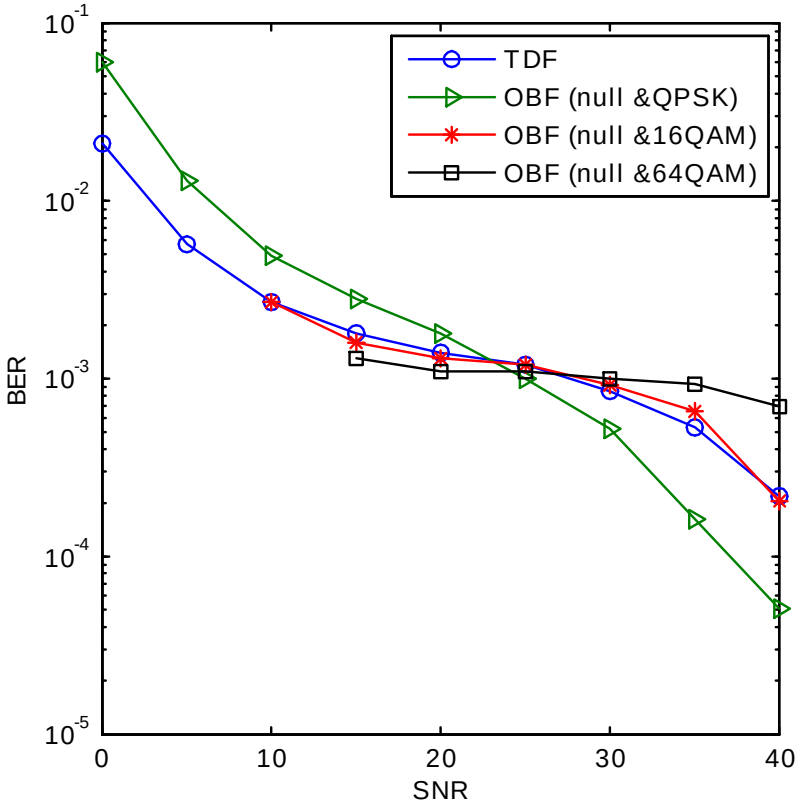

Figure 5.14. Comparison between time-domain feedback technique and one bit feedback technique in terms of BER (p=10^{-5}).

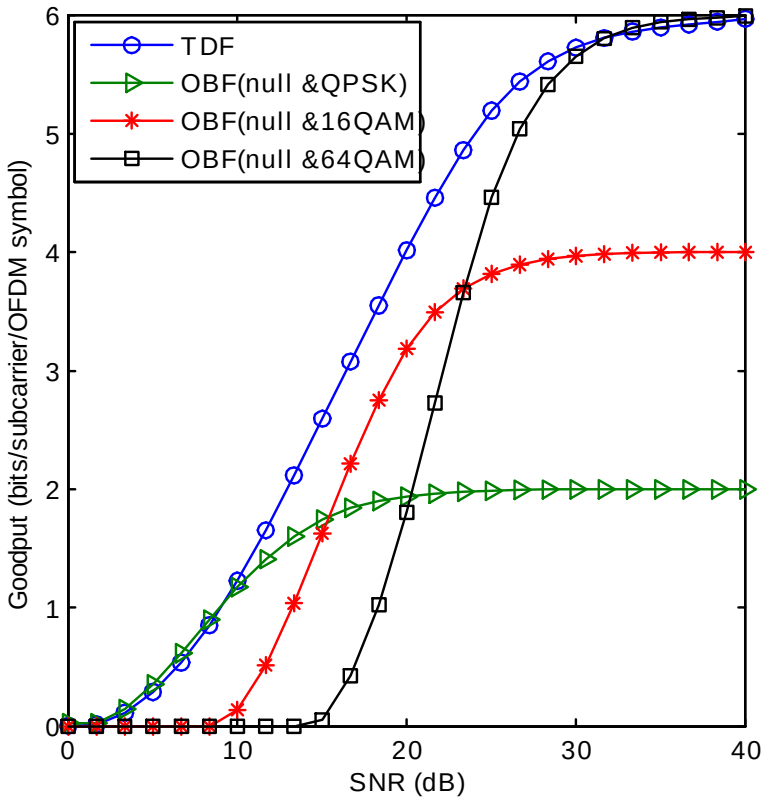

Figure 5.15. Comparison between time-domain feedback technique and one bit feedback technique in terms of goodput (p=10^{-5}).

CHAPTER 6

CONCLUSIONS AND FUTURE WORK

6.1 Summary and Conclusions

End-to-end performance evaluation of link adaptation of OFDM wireless communication systems over limited feedback channel is the main concern of the thesis. System adaptation gaines a great attention in this work in order to be able to pursue channel variations and optimize the transmission parameters to have a reliable communication accordingly. Link adaptation is performed at the transmitter side through adaptive modulation algorithm where the transmitter receives CSI from the receiver side through feedback channel and the modulation order of each of the OFDM subcarriers is adapted according to BER constraints.

Accurate CSI should be available at the receiver side through channel estimation to have high performance link adaptation process. It is considered as a challenging problem in wireless systems due to time and frequency selectivity of wireless channels. Pilot-aided channel estimation technique is used in the thesis over a static and mobile frequency selective channels and its impact on the system performance is evaluated.

The feedback channel is usually limited in terms of the transmission rate due to power and bandwidth limitations. One of the main contributions of the thesis is developing a new feedback technique with reduced overhead cost and can achieve a reliable adaptive communication system. In the proposed feedback overhead reduction technique, a truncated and quantized version of the channel impulse response is fed back to the transmitter where the average number of bits in feedback overhead is limited to one bit per subcarrier. Consequently, the total number of overhead bits is limited to N bits. At the transmitter side,

FFT operation is used across all subcarriers to generate the channel frequency response. The performance of the proposed feedback technique is evaluated over a feedback channel that experiences errors and delay, so the feedback information might be erroneous and outdated. The quantization of the feedback vector, is also considered in system model. The performance is evaluated over a range of quantization bits number, probability of error in the feedback channel and mobility in the feedforward channel. The proposed feedback technique is compared to several feedback techniques and its performance is proved to outperform the other techniques in terms of throughput and BER while using a reduced feedback overhead.

6.2 Future Work

The results of the thesis provide a strong foundation for future work. It points to a variety of interesting future directions. One of these directions is evaluating the performance of the proposed system analytically. Another possible direction is related to 2-dimension interpolation in pilot-aided channel estimation process where pilot grid can be designed in time domain as well as frequency domain. Moreover, investigating and developing techniques to estimate the channel information at the transmitter side is an interesting future direction, as it can improve adaptation quality, specialy in the presence of mobility in wireless communication channels.

BIBLIOGRAPHY

[1] M. Kalil, A. Shami and A. Al-Dweik, "QoS-Aware Power-Efficient Scheduler for LTE Uplink. " *IEEE Trans. Mobile Computing*, vol. xx, Oct. 2014.

[2] Mobile WiMAX-Part, Mobile. "I: A technical overview and performance evaluation." WiMAX Forum. 2006.

[3] E. Hossain, M. Rasti, H. Tabassum, and A. Abdelnasser. "Evolution toward 5G multi-tier cellular wireless networks: An interference management perspective." *IEEE Wireless Communications*, vol. 21, no. 3 pp: 118-127, June 2014.

[4] X. Duan, and X. Wang. "Authentication handover and privacy protection in 5G hetnets using software-defined networking." *IEEE Communications Magazine*, vol. 53, no.4 pp: 28-35, April 2015

[5] Y. Liu, W. Chen, and X. Huang. "Capacity based adaptive power allocation for the OFDM relay networks with limited feedback.", 2011 *IEEE International Conference on Communications (ICC)*, 2011.

[6] E. Choi, W. Choi, J. Andrews, and B. Womack, "Power loading using order mapping in OFDM systems with limited feedback," IEEE Signal Process. Lett., vol. 15, pp. 545-548, 2008

[7] K. Kyungchul, S. Lee, H. Min, S. Choi, and D. Hong. "New OFDM channel estimation with dual-ICI cancellation in highly mobile channel." *IEEE Trans. Wireless Comm.,* vol. 9, no. 10 pp: 3155-3165, Oct. 2010.

[8] "Air interface specifications", Wimax Forum, 2013.

[9] L. Dawoon, M. Choi, and S. Choi. "Channel estimation and interference cancellation of feedback interference for DOCR in DVB-T system." , *IEEE Trans. Broadcasting*, vol. 58, no.1 pp: 87-97, March, 2012.

[10] P. Ladislav, and T. Kratochvil. "DVB-H and DVB-SH-A performance and evaluation of transmission in fading channels." *IEEE International Conference on Telecommunications and Signal Processing (TSP), 34th*, 2011.

[11] D. Bueche, P. Corlay, M. Gazalet, and F. Coudoux. "A method for analyzing the performance of comb-type pilot-aided channel estimation in power line communications." *IEEE Trans. Consumer Electronics*, vol. 54, no. 3 pp: 1074-1081, Aug. 2008

[12] Ye Li, and Gordon L. Stuber. *Orthogonal frequency division multiplexing for wireless communications*. Springer Science & Business Media, 2006.

[13] S. Coleri, M. Ergen, A. Puri, and A. Bahai. "Channel estimation techniques based on pilot arrangement in OFDM systems." *IEEE Trans. Broadcasting*, vol. 48, no. 3, pp: 223-229, Sep. 2002.

[14] D. Wang, Y. Cao, and L. Zheng, "Efficient two-stage discrete bit-loading algorithms for OFDM systems,"*IEEE Trans. Vehicular Tech*, vol. 59, no. 7, pp. 3407–3416, Sep. 2010

[15] D. Wang, Y. Cao, L. Zheng and Z. Du, "Iterative Group-by-Group Bit-Loading Algorithms for OFDM Systems," *IEEE Trans. Vehicular Tech*, vol. 62, no. 8, pp. 4131–4135, Oct. 2013

[16] A. M. Wyglinski , F. Labeau and P. Kabal, "Bit loading with BER-constraint for multicarrier systems", *IEEE Trans. Wireless Comms.*, vol. 4, no. 4, pp.1383 -1387, July 2005

[17] L. Piazzo. "Optimal fast algorithm for power and bit allocation in OFDM systems." *IEEE Trans. Vehicular Tech,* vol. 60, no.3, pp.1263-1265, March 2011

[18] N. Papandreou and T. Antonakopoulos, "A new computationally efficient discrete bit-loading algorithm for DMT applications.", *IEEE Trans. Comms.*, vol. 53, no. 5, pp. 785–789, May 2005

[19] K. Liu and B. Tang, "Adaptive power loading based on unequal-BER strategy for OFDM systems.", *IEEE Commun. Lett.*, vol. 13, no. 7, pp. 474–476, Jul. 2009

[20] Ming Lei, H. Harada, H. Wakana and Ping Zhang, "An adaptive power distribution algorithm for improving spectral efficiency in OFDM," *IEEE GLOBECOM 2004*, vol. 6, pp. 3716-3720, Dec. 2004

[21] K Liu, B Tang and Y Liu. "Adaptive power loading based on unequal-ber strategy for OFDM systems" , *IEEE Communication Letters*, no.7.vol.13, pp.474-476, Jul. 2009

[22] Amin, Osama, and Murat Uysal. "Adaptive power loading for multi-relay OFDM regenerative networks with relay selection." *IEEE Trans. Comms.*, vol. 60n no.3, pp. 614-619, March 2012

[23] A. Lozano, A.Tulino and S. VerdÃº, "Optimum power allocation for parallel Gaussian channels with arbitrary input distributions", *IEEE Trans. Inform. Theory*, vol. 52, pp.3033 -3051, Jul. 2006

[24] Yang Qi, W. Shieh, Ma Yiran, "Bit and Power Loading for Coherent Optical OFDM", *IEEE Photonics Technology Letters*, vol.20, no.15, pp.1305-1307, Aug. 2008

[25] Bedeer, Ebrahim, et al. "A novel algorithm for joint bit and power loading for OFDM systems with unknown interference.", 2012 *IEEE International Conference on Communications (ICC)*. IEEE, 2012.

[26] N. Papandreou and T. Antonakopoulos "A new computationally efficient discrete bit-loading algorithm for DMT applications", *IEEE Trans. Comms*, vol. 53, no. 5, pp.785 -789, May 2005

[27] Amin, Osama, and Murat Uysal. "Optimal bit and power loading for amplify-and-forward cooperative OFDM systems." *IEEE Trans. Wireless Comms.*, vol. 10, no. 3, pp. 772-781, March 2011

[28] T. N. Vo, K. Amis, T. Chonavel, P. Siohan, "Achievable Throughput Optimization in OFDM Systems in the Presence of Interference and its Application to Power Line Networks."*IEEE Trans. Comms.*, vol. 62, no. 5, pp.1704-1715, MAY 2014

[29] Bedeer, Ebrahim, et al. "Constrained joint bit and power allocation for multicarrier systems." *Global Communications Conference (GLOBECOM)*, 2012 IEEE. Dec. 2012

[30] A. Wyglinski, F. Labeau, and P. Kabal. "Bit loading with BER-constraint for multicarrier systems." *IEEE Trans. Wireless Comms.,* vol. 4, no.4, pp: 1383-1387, July 2005.

[31] B. Sklar, Digital Communications Fundamentals and Applications, Second Edition. Prentice-Hall, 2008

[32] A. Goldsmith, *Wireless communications*, New York : Cambridge University Press, 2005.

[33] Sigen Ye, R. S. Blum and L. J. Cimini "Adaptive OFDM systems with imperfect channel state information." *IEEE Trans. Wireless Comms.,*vol. 5, no.11, pp: 3255-3265, Nov. 2006.

[34] S. Akoum, and R. Heath. "Limited feedback for temporally correlated MIMO channels with other cell interference." *IEEE Trans. Signal Process.* vol. 58, no. 10, pp: 5219-5232, Oct. 2010.

[35] A. Al-Dweik, F. Kalbat, S. Muhaidat, O. Filio and S. M. Ali. "Robust MIMO-OFDM System for Frequency-Selective Mobile Wireless Channels" *IEEE Trans. Vehicular Tech,* vol. xx, no.y, pp.1-12, 2014.

[36] Su, Yongtao, et al. "Robust downlink precoding in multiuser MIMO-OFDM systems with time-domain quantized feedback." *Wireless Communications and Networking Conference (WCNC),* 2010 IEEE. IEEE, 2010.

[37] Liu, Yong, Wen Chen, and Xiaopeng Huang. "Capacity based adaptive power allocation for the OFDM relay networks with limited feedback." *(ICC), 2011 IEEE International Conf. Comm.*, 2011.

[38] Hajiaghayi, Mahdi, Min Dong, and Ben Liang. "Using limited feedback in power allocation design for a two-hop relay OFDM system." . *ICC'09. IEEE International Conf. Comm.* IEEE, 2009.

[39] Rong, Yue, Sergiy A. Vorobyov, and Alex B. Gershman. "Adaptive OFDM techniques with one-bit-per-subcarrier channel-state feedback." *IEEE Trans. Comms*, vol. 57,no 11, pp.1993-2003, Nov. 2006.

[40] M. Agarwal, D. Guo and M. Honig. "Limited-Rate Channel State Feedback for Multi-carrier Block Fading Channels" *IEEE Trans. Info. Theory*, vol. 56, no. 12, Dec. 2010.

[41] B. Mondal and R. W. Heath, Jr., "Channel adaptive quantization for limited feedback MIMO beamforming systems," *IEEE Trans. Signal Process.*, vol. 54, no. 12, pp. 4731-4740, Dec. 2006.

[42] L. Wan, X. Zhong, Y. Zheng, and S. Mei, "Adaptive codebook for limited feedback MIMO system," i*n Proc. Wireless and Opti. Comm. Networks (WOCN'09) 2009*, Apr. 2009.

[43] V. Lau and T. Wu "Optimal Transmission and Limited Feedback Design for OFDM/MIMO Systems in Frequency Selective Block Fading Channels" *IEEE Trans. Wireless Comm.*, vol. 6, no. 5, p: 1569-1573, May 2007

[44] Zhou, Mingxin, Leiming Zhang, Lingyang Song, and Merouane Debbah. "A Differential Feedback Scheme Exploiting the Temporal and Spectral Correlation." *IEEE Trans. Vehicular Tech.*,vol. 62, no. 9, pp.4701-4707, Nov. 2013

[45] Wang, J., et al. "A Dynamic Region based Limited Feedback Scheme for Efficient Power Allocation in OFDM Systems." *IEEE Communications Letters,* vol. 17,no. 11, pp.2036-2039, Nov. 2013

[46] Marques, Antonio G., et al. "Optimizing average performance of OFDM systems using limited-rate feedback." *IEEE Trans. Wireless Comm.,* vol. 9, no.10, pp.3130-3143, Oct. 2010

[47] Eslami, Mohsen, and Witold A. Krzymien. "Net throughput maximization of per-chunk user scheduling for MIMO-OFDM downlink." *IEEE Trans. Vehicular Technology,* vol. 60, no. 9, pp. 4338-4348, Nov. 2011

[48] He, Y., and Subhrakanti Dey. "Throughput Maximization in Poisson Fading Channels with Limited Feedback." *IEEE Trans. Comm.*, vol. 61, no.10, pp. 4343-4356, Oct 2013

[49] Liu, Yong, and Wen Chen. "Limited-feedback-based adaptive power allocation and subcarrier pairing for OFDM DF relay networks with diversity." *IEEE Trans. Vehicular Technology*, vol.61, no.6 , pp. 2559-2571, July 2012

[50] El Ayach, Omar, and Robert W. Heath. "Grassmannian differential limited feedback for interference alignment." *IEEE Trans. Signal Processing*, vol. 60, no.12, pp. 6481-6494, Dec. 2012

[51] Huang, Yongming, et al. "Exploiting long-term channel correlation in limited feedback SDMA through channel phase codebook." *IEEE Trans. Signal Processing*, vol. 59, no.3, pp. 1217-1228, March 2011

[52] Ma, Yao, et al. "Error performance of transmit beamforming with delayed and limited feedback." *IEEE Trans. Wireless Comms.*, vol. 8, no 3, pp. 1164-1170, March 2009

[53] Huang, Kaibin, Robert W. Heath, and Jeffrey G. Andrews. "Limited feedback beamforming over temporally-correlated channels." *IEEE Trans. on Signal Processing*, vol. 57, no 5, pp: 1959-1975, May 2009

[54] Bhagavatula, Ramya, and Robert W. Heath. "Predictive vector quantization for multicell cooperation with delayed limited feedback." IEEE Trans. on Wireless Comms., vol. 12, no 6 pp: 2588-2597, June 2013

[55] Lamahewa, Tharaka A., et al. "Model-based pilot and data power adaptation in psam with periodic delayed feedback." *IEEE Trans. on Wireless Comms.*, vol. 8, no 5 pp: 2247-2252, May 2009